RECOVERY OF ZINC FROM AQUEOUS SOLUTION

NICHOLAS YAP JUNMIN

A project report submitted in partial fulfilment of the requirements for the award of the degree of Bachelor (Hons.) of Chemical Engineering

Lee Kong Chian Faculty of Engineering and Science
Universiti Tunku Abdul Rahman

May 2016

DECLARATION

I hereby declare that this project report is based on my original work except for citations and quotations which have been duly acknowledged. I also declare that it has not been previously and concurrently submitted for any other degree or award at UTAR or other institutions.

Signature : Nicholas

Name : Nicholas Yap Junmin

ID No. : 11UEB05228

Date : 12th May 2016

APPROVAL FOR SUBMISSION

I certify that this project report entitled **"RECOVERY OF ZINC FROM AQUEOUS SOLUTION"** was prepared by **NICHOLAS YAP JUNMIN** has met the required standard for submission in partial fulfilment of the requirements for the award of Bachelor of Engineering (Hons.) Chemical Engineering at Universiti Tunku Abdul Rahman.

Approved by,

Signature : _____

Supervisor : Dr. Gulnaziya Issabayeva

Date : _____

Specially dedicated to
my beloved family, lecturers and friends

ACKNOWLEDGEMENTS

I would like to thank everyone who had contributed to the successful completion of this project. I would like to express my gratitude to my research supervisor, Dr. Gulnaziya Issabayeva for her invaluable advice, guidance and her enormous patience throughout the development of the research.

Besides, I would like to express my utmost thanks to my loving parents and all my friends who had helped and given me the encouragement that I needed from the beginning till the completion of this project.

Lastly but not least, I would like to thank all the laboratory officers in the Department of Chemical Engineering for their kind assistance during the project.

RECOVERY OF ZINC FROM AQUEOUS SOLUTION

ABSTRACT

This research project evaluated the recovery of zinc through application of adsorption, desorption and electrochemical deposition methods. The adsorption experiments were carried out using synthetic stock solution of 0.01 M $Zn(NO_3)_2$ and granular palm shell activated carbon (PSAC). 0.1 M and 0.2 M of hydrochloric and nitric acid along with 0.2 M and 0.5 M of citric acid were used to desorb the adsorbed zinc ions to prepare electrolyte solutions for the zinc electrodeposition tests. The adsorption results showed that the adsorption capacity increased when initial zinc ions concentration increased from 10 to 100 ppm with maximum adsorption efficiency of 98 %. The highest desorption efficiency was achieved for 0.1 M HCl. The higher acid concentration has led to a decrease of desorption efficiency for HCl and $C_6H_8O_7$ but differed for HNO_3. The respective solutions with desorbed zinc ions were subjected to cyclic voltammetry (CV) tests. The chloride-based electrolyte showed the best electroreduction behaviour of zinc with a sharp peak, followed by nitrate-based electrolyte showing a wider peak and lastly citrate-based electrolyte with no peak at all. In the subsequent electrodeposition experiments, chloride-based electrolyte was found to yield the highest zinc deposition. It was observed that higher concentration of the desorbing agents lowered the deposition efficiency; however, higher zinc concentration improved deposition efficiency due to greater mass transfer. In conclusion, the electrodeposition of zinc was successful achieving effective reduction of zinc ions concentration to meet the maximum permissible limit of zinc in wastewater of 2 ppm at the varied deposition time and applied current density parameters.

TABLE OF CONTENTS

LIST OF TABLES

LIST OF FIGURES

LIST OF SYMBOLS / ABBREVIATIONS

C_0	initial metal ions concentration, mg/L
C_t	effluent metal ions concentration, mg/L
K_{sp}	Solubility product constant
m	Mass, g
t	time, min

BR	Britton-Robinson
CV	Cyclic Voltammetry
DC	Direct Current
DOE	Department of Environment
EDX	Energy Dispersive X-Ray
ICP-OES	Inductively Coupled Plasma-Optical Emission Spectroscopy
ILZSG	International Lead and Zinc Study Group
MPOC	Malaysia Palm Oil Council
PSAC	Palm Shell Activated Carbon
RVC	Reticulated Vitreous Carbon
SCE	Saturated Calomel Electrode
SEM	Scanning Electron Microscopy
SHE	Standard Hydrogen Electrode
WHO	World Health Organization
XRD	X-ray Powder Diffraction

CHAPTER 1

INTRODUCTION

1.1 Heavy metal pollution

In the past few decades, the expeditious industrialization has contributed to the existing level of environmental pollution, especially water pollution. The effluents generated from miscellaneous industries such as mining, metal smelting, electroplating, paper industries and so on are reported to contain enormous amount of hazardous pollutants such as dye, heavy metals, pesticides and suspended solids (Srivastava, Mall and Misha, 2006). Heavy metals are categorized as hazardous pollutants owing to their adverse environmental and health effects even at low concentration.

Heavy metals present in industrial wastewater in various forms such as soluble, insoluble, organic, inorganic, oxidized, reduced, precipitated, adsorbed, complexed and as free metals. Heavy metals such as nickel, iron, lead, zinc, cadmium and copper pose a serious threat to the environment through the contamination of surface water, groundwater and sea water (Konstantinos, Achilleas and Valsamidou, 2011). They are highly toxic, non-biodegradable and carcinogenic to human beings as well as to the plants and animals.

Heavy metals tend to bioaccumulate in living organisms. One of the most compelling evidences is the impact of excessive amount of copper intake on plants and algae (Almamoori, Hassan and Kassim, 2012). Copper is necessary for plants

and algae. However, a surplus of copper leads to the inhibition of photosynthesis and damage to plasma membrane of the plant cells. As for human, the containment of heavy metals in drinking water imparts various cardiovascular diseases and impairment of nervous system. Water contamination is responsible for 70-80 % of the illnesses detected among children and women (World Health Organization, 2000). The impacts of heavy metals on humans along with the sources of emission are shown in Table 1.1. It shows that the inhalation of zinc fumes leads to "zinc fever", a fever accompanied with chilling effect in human (Gupta and Sharma, 2003). Apart from that, fumes from zinc chloride may cause fatalities due to neuronal cell death.

As a result of significant impact on public health, removal of heavy metals from industrial effluents is crucial to maintain clean and safe water resources. Zinc for example is of major concern from the toxicity perspective. Stringent legislations are implemented to reduce the amount of zinc discharged into water sources. In Malaysia, the release of heavy metals to water bodies is in compliance with Standard A and Standard B according to Department of Environment (2012) as shown in Table 1.1 for the respective heavy metals. The permissible limits in industrial effluents is 2.0 mg/L. This limit must be adhered by industries before discharging the effluent to the environment.

In spite of its detrimental effects on humans, zinc metal is still one of the widely used metals with a myriad of practical usages. Zinc is vital for biochemical functions in various metabolism pathways such as cell replication in humans, gene expressions in animals and most importantly, cell division in plants. (Li, Xiang and Tong, 2008). Approximately 40 % of zinc metal has been utilized to galvanize iron and other metals for preventing corrosion as shown in Figure 1.1. Another important application of zinc is the manufacture of zinc oxide.

Table 1.1: Permissible limits and health effects of heavy metals (DOE, 2012)

Heavy Metal	Major Source of Emission	Permissible limits for industrial effluent discharge (mg/L)		Permissible limits for drinking water (mg/L)	Effect on Human Health
		A*	B*	WHO	
Arsenic	Insecticides, metal smelting, volcanic activity	0.05	0.10	0.01	Cardiovascular diseases, haematopoiesis, peripheral neuropathy
Cadmium	Electroplating, smelter slags and wastes	0.01	0.02	0.003	Anaemia, encephalopathy, hepatitis and nephritic syndrome
Copper	Electroplating, mining industries	0.2	1.0	2	Diarrhea, dizziness, stomachache
Lead	Painting, car batteries	0.1	0.5	0.01	Anemia, damage to the nervous system, gastrointestinal symptoms
Mercury	Pesticide additives, batteries, paper industries	0.005	0.05	0.006	Damage reproduction in mammals
Nickel	Incineration of waste and sewage, non-ferrous metal smelters	0.2	1.0	0.07	Chronic bronchitis, reduction in lung function, nasal sinus
Zinc	Smelter slags and wastes, bottom fly ash	2.0	2.0	3	Short-term illness (i.e. metal fume fever), restlessness, edema, neuronal death

A* and B* are applicable for sources of drinking water and for effluent discharge, respectively.

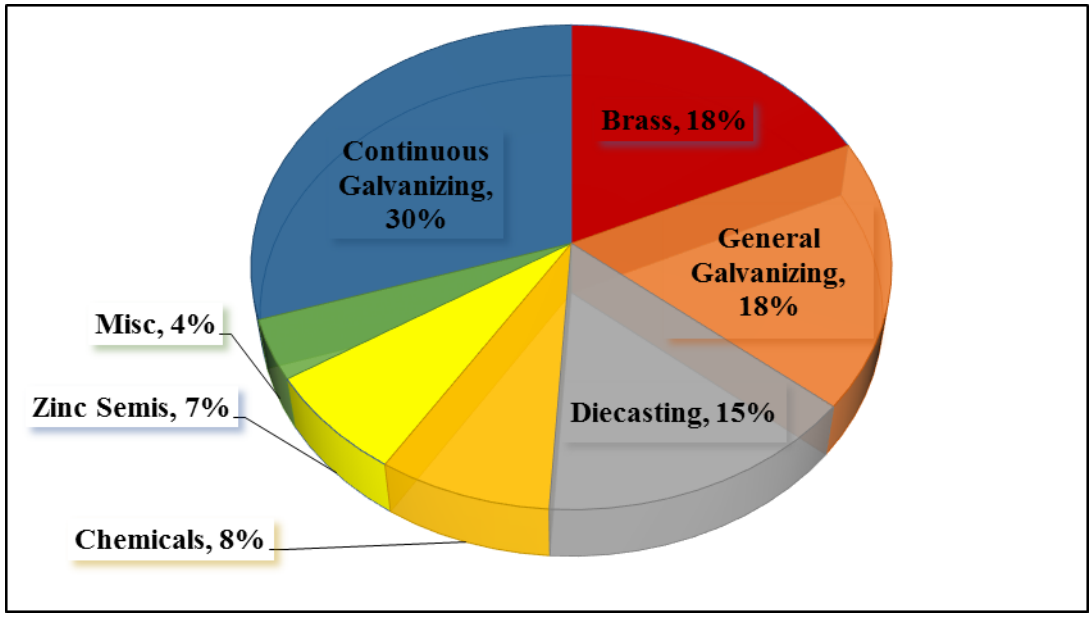

Figure 1.1: Applications of Zinc in various processes (Moezzi, McDonagh and Cortie, 2012)

The captivating properties of zinc oxide have gathered interests of researchers from various industries. Zinc oxide has a large electron binding energy of 60 meV at room temperature, enabling zinc oxide to produce electronic devices that operate perfectly at room temperature (Ahmed, et al., 2013). Besides, zinc oxide has good photoconductivity properties, and is therefore used for photocopying. Additionally, 50 % of zinc oxide is used in the rubber industry, serving as a vulcanizing activator to enhance the effectiveness of vulcanization process through the formation of three dimensional cross-linking between chains of rubber molecules to improve rubber elasticity (Zhang, 1996).

It has been foreseen that zinc oxide is to have a huge market outlook in Malaysia resulting from worldwide demands for rubber. Malaysia was one of the top three natural rubber exporters in 2013 (International Trade Centre, 2014). Table 1.2 shows that Malaysia exported around $ 2,230,998,000 of natural rubber in terms of dollar value constituting 9.6 % of the total rubber exports in 2013. With such a huge demand for natural rubber, the research work on zinc oxide in surface chemistry, synthesis techniques and condensed matter physics is given much attention (Ahmed, et al., 2013).

Table 1.2: Top ten countries exporting natural rubber in 2013 (International Trade Centre, 2014)

Country	Dollar worth of natural rubber	Total export (%)
Thailand	$8,233,510,000	35.4
Indonesia	$6,910,663,000	29.7
Malaysia	$2,230,998,000	9.6
Vietnam	$1,810,216,000	7.8
Côte d'Ivoire	$ 942,518,000	4.0
Germany	$336,816,000	1.4
Belgium	$296,008,000	1.3
Guatemala	$238,843,000	1.0
Liberia	$201,998,000	0.9
Myanmar	$199,618,000	0.9

A new technology must be developed to remove and recover zinc from industrial wastewater. An equilibrium point will be achieved following the invention of new technology where the level of zinc can be minimized below its' permissible limits and utilizing the surplus of zinc for other applications, for instance zinc oxide in rubber industry. Likewise, removal and recovery of zinc from industrial wastewater has to be economically feasible and environmental friendly as a basis for sustainable development in Malaysia.

1.2 Zinc removal and recovery

There are various methods of removal of heavy metals from industrial wastewater such as filtration, membrane, separation, ion exchange, chemical precipitation, electrodeposition and adsorption (Volesky, 1995). Among aforementioned treatment technologies, adsorption is one of the most widely used separation and purification method due to its great efficiency, high selectivity and low operating cost. It is

governed by several important parameters mainly pH, contact time, temperature and so on.

The choice of sorbent is another major parameter to be considered. There are four major types of generic sorbents have been adopted for the commercial use of adsorption such as activated carbon, zeolites, silica gel and activated alumina (Yang, 2003). The most commonly used sorbent in the removal of heavy metals is activated carbon. The good sides of the activated carbon are high surface area and large pore volume with high porosity. However, due to the high cost of activated carbon, the application of it in industries is restricted. Different low cost precursors, agricultural wastes termed as green adsorbent have been investigated by the researchers to replace the use of the conventional activated carbon (Kyzas and Kostoglou, 2014). For instance corn cubs, wasted tea leaves, hazelnut shells, almond shells, sugar cane and palm shells (Reddad, et al., 2002; Issabayeva, Aroua and Sulaiman, 2006). In general, low cost adsorbent should require minimal processing and be vastly available in nature.

The use of sorbents for adsorption process depends on the local availability. In Malaysia, significant volume of waste is generated from palm oil industry annually triggering environmental and disposal problems (Issabayeva, Aroua and Sulaiman, 2006). Palm oil wastes are either burnt in open air or dumped in areas in vicinity of the mill. This scenario was initiated by the huge market share of global palm oil needs, nearly 44 % of the world's export (Malaysia Palm Oil Council, 2014). Huge market share by Malaysia has led to a greater palm oil production, in turn causing more palm oil wastes to be generated. The palm oil wastes such as palm kernel, palm shell and palm husk are used to prepare activated carbon.

The adsorbents can be regenerated through desorption step to maximize its usage. This is to economize the adsorption process. Desorption step is applicable through the use of desorbing agent with mostly acid to strip the adsorbed zinc from adsorbent and bring it back to the solution. By doing it, sludge volume is expected to be minimized as it has been proven by most of the literature studies on the potential to recover zinc from desorption medium (Gupta and Ali, 2004; Ye, Zhu and Du,

2010; Hesas, et al., 2013). In addition, regeneration of spent adsorbent allows zinc to be recovered in the desorbing solution in concentrated form.

Many researchers focused on alternatives to enhance adsorption and desorption efficiency. However, there is little experimental work is done on the handling of desorbed metal in industries. The recovery of zinc metal from desorption medium aims to reduce resource wastage, disposal and material cost. Electrochemical process is one of the alternatives as compared to conventional treatment technologies for example ion exchange, precipitation, sol-gel, and adsorption to recover zinc ion from desorption solution. Besides, additional advantages of the electrochemical process were mentioned by Galla, Juttner and Schmieder (2000) in their own literature which are versatility, energy efficiency, amenability to automation and cost effectiveness. These are the reasons on why the electrochemical process has becoming a prospect to recover heavy metals from industrial effluents. An increase of the application of electrochemical process are clearly shown in decolourization of wastewaters, deodorization of wastewaters, disinfectation of water and recovery of metal ion from industrial effluent (Stankovic´, 2012). Hence, electrochemical process, specifically electrodeposition is utilized to recover zinc metal from desorption step.

1.3 Problem Statement

It has been shown that the principles of electrochemistry can be well implemented in the recovery of zinc metal to its pure metallic form through cathodic reduction on the substrate (Mendoza-Huizar, Rios Reyes and Gomez-Villegas, 2010). However, it requires thorough control over the parameters such as temperature, pH, current density and so on to optimize efficiency and quality of recovered metal. Overall, the selection of electrochemical process to be part of the treatment process to recover zinc is economically viable considering the merits and demerits of each treatment technologies.

Removal and recovery of zinc from industrial effluent is the main agenda of this project which is to be accomplished through application of suitable processes, i.e. adsorption-desorption-electrochemical. Such approaches have not been studied before and require careful monitoring of the parameters of each involved process at a time. The three-step process presents environmental and economical benefits as it utilizes palm oil industry waste based adsorbent and recycling of valuable metal resources.

1.4 Objectives of research

The focus of the research was to remove and recover zinc from synthetic wastewater through the combination of adsorption, desorption and electrochemical reaction steps. In this research, the specific objectives were to investigate:

1. The efficiency of desorbing agent to strip zinc ions from palm shell activated carbon.
2. The electroreduction behaviour of zinc ions in different type of electrolytes using cyclic voltammetry technique.
3. The effect of zinc concentration on the efficiency of zinc deposition.
4. The effect of deposition period and applied current density on the zinc deposition.

1.5 Scope of study

The following scope of work was planned to achieve the research objectives.

1. Preparation of adsorbent which was palm shell activated carbon.
2. Adsorption/Desorption experiments using synthetic wastewater containing zinc ions.

3. Cyclic Voltammetry (CV) tests to determine electroreduction potential of zinc in a range of zinc solutions of different concentrations; and evaluation of the additives effect on the process.
4. Chronopotentiometry tests to deposit zinc from synthetic wastewater under varying parameters of current density, reduction potential and deposition duration.

CHAPTER 2

LITERATURE REVIEW

2.1 Properties and Applications of Zinc

Zinc is an almost omnipresent type of metal which plays a pivotal role in various physiological processes and prevention of many diseases. Besides, zinc is one of the natural components in Earth's crust. Amongst all the elements in the Earth's crust, zinc is ranked in 23rd in terms of relative abundance, accounting 0.013 % as compared to iron's 5.0 % and aluminium's 8.13 %. The average level of zinc is 70 mg/kg on the basis of dry weight in the Earth's crust. It is also the world's fourth vastly used metal for worldwide production and usage, ranked right behind iron, aluminium and copper (Morrow, 1986).

Zinc is a transition amphoteric metal located in the fourth period, Group 2B in the periodic table with atomic number of 30. It has two oxidation states, Zn (0) and Zn (+2). There are few important zinc natural minerals such as sphalerite, smithsonite and hemimorphite found as ores. Zinc forms various types of compounds, zinc chloride, zinc oxide and zinc sulphate (International Lead and Zinc Study Group, 2015).

Pure zinc has a characteristic silvery blue metallic colour, low melting point (419 °C) and boiling point (908 °C). Transition metals are generally ductile, malleable and able to conduct electricity and heat easily (Zhang, 1996). In a non-

scientific term, zinc is called as “spelter”. It is fairly reactive combining with oxygen and other non-metals.

The captivating chemical and physical properties of zinc has led to numerous applications of zinc in various types of industries. Table 2.1 shows that zinc metal is continuously mined with an increasing trend from 12360000 tonnes to 13280000 tonnes in the period from 2010 to 2014. International Lead and Zinc Study Group (2015) forecasted the global demand of zinc in various industries will increase by 3.7 % to 14.14 million tonnes beyond 2015.

Table 2.1: Zinc Supply and Usage Worldwide from 2010–2015 (International Lead and Zinc Study Group, 2015)

000 tonnes	2010	2011	2012	2013	2014	2015			
						Jan	Feb	Mar	Apr
Mine Production	12360	12584	12900	12982	13280	1109.4	1080.0	1134.6	1152.2
Metal Production	12896	13064	12630	12872	13304	1178.9	1092.7	1157.0	1175.0
Metal Usage	12628	12679	12368	12956	13521	1130.6	986.1	1136.5	1169.6

According to Statista (2015), the consumption of zinc worldwide reached 13.6 million metric tons in 2014. The consumptions of zinc are categorized to six major groups as follows:

i. Zinc coatings

The classification of various categories of zinc and zinc alloy coatings is in accordance to the composition of the coating and production techniques. In terms of chemical composition, the zinc based coatings are sorted into few major groups such as pure zinc, zinc-aluminium, zinc-iron and zinc composites (Zhang, 1996). Production method employed are hot dipping, electroplating, sherardizing and metallizing. The typical uses of zinc and zinc alloy coating are shown in Table 2.2.

The main use of zinc is as a coating for corrosion protection. This is due to the position of zinc respective to iron in the electromotive series.

Table 2.2: Typical Applications of Zinc Coating Products (Zhang, 1996)

Type of coating	Applications
Zinc- Aluminium	Roofing, tailpipes, heat shields, chimneys.
Zinc - Cobalt	Automotive small parts and fasteners.
Zinc - Iron	Structural components and autobody panels.
Zinc - Nickel	Structural components, housings, appliances, fasteners.

ii. Cast alloys

Cast alloys are usually manufactured through die-casting method. This method is a high speed operation that requires no final shaping. The products from the die-casting operation are utilized for automotive compartments, household appliances, building hardware and so on. The relatively high aluminium content of 4.0 % is the main contributor to the alloys' excellent castability and strength (Zhang, 1996).

iii. Alloying elements in brass and other type of alloys

The predominant use of zinc as an alloying element is reflected in several other alloy systems. For instance, the formation of brasses and bronzes through the mixture of zinc and copper in the alloy system constitutes 30–40 wt % of the overall alloy composition (Zhang, 1996). The addition of zinc to copper enhances the overall strength of the material leading to a wide range of applications in engineering field. One of the main application of brass is resilient protection towards pitting corrosion and stress corrosion cracking under the extreme weather and water environment.

iv. Wrought zinc alloy

Wrought zinc alloys are obtained in the form of rolled strip, sheet, extruded rod and shape. Wrought zinc alloys are strictly for structural applications owing to the tendency of the alloys to creep at room temperature. One of the main purposes for wrought zinc alloys is drawn battery cans. Wrought zinc alloys are commercialized due to its huge potential in diverse areas such as architecture, automobiles, and low-volume rechargeable batteries for propulsion (Zhang, 1996).

v. Zinc oxide

Zinc oxide is characterized by great chemical stability and high electrochemical coupling coefficient (Radzimska and Jesionowski, 2014). Zinc oxide is classified as semiconductor material in group II-VI with its covalence on the boundary between ionic and covalent semiconductors. It can be used as energy generator and sensor as a result of its piezoelectric and pyroelectric properties. Besides, it is used to enhance the thermal conductivity of the products from rubber derivative.

vi. Zinc powder

Particulate materials specifically zinc dust and zinc powder are products from zinc metal. The term “dust” is usually used for fine particles that are ranging 2 – 20 μm in diameter and “powder” for coarser particles. Basically, zinc dust is produced by the condensation of zinc vapour; whereas zinc powder is produced from the product of atomization of molten zinc in the presence of air or under the inert condition. The main applications of these zinc-based products are as reagents for the preparation of chemicals, metal refining processes and as an active ingredient for zinc batteries.

2.2 Adsorption of zinc

The application of adsorption was initiated at the end of 18th century to get rid of unpleasant odour using dusted wounds with powdered charcoal as adsorbent. At present, adsorption is a well-established technology for the removal of heavy metals due to high efficiency and low cost. Adsorption is governed by either Van der Waals interactions (physical adsorption) or chemical process (chemisorption) depending on the nature of forces (Dabrowski, 2001). Physical adsorption is a reversible process arising from the intermolecular force of attraction between molecules of the adsorbent and adsorbate. While for chemisorption, it takes place due to the chemical interaction between the solid and the adsorbate. Several important parameters have to be accounted prior to adsorption process such as pH, adsorbent dosage, temperature, contact time, concentration of adsorbate and type of adsorbent. These parameters influence the three major steps of adsorption mechanism: external mass transfer, intraparticle diffusion and adsorption at an interior side.

pH of the solution plays an important role in the adsorption of metal ions in view of speciation of metal ions. Ferro-Garcia, et al. (1988) investigated the adsorption of zinc ions on three different agro-based activated carbons namely almond shells, olive stones and peach stones under different pH values. The results showed that removal of zinc ions was negligible below pH 2. The adsorbents' surfaces were positively charged and resulted in a repulsive electrostatic interaction between its' surface and zinc ion. At higher pH values, an exchange of hydrogen ion between the carbon surface with zinc ions, resulting in an enhancement in zinc ions uptake. This reflects the importance of pH in affecting the uptake of zinc ions.

The effect of adsorbent dosage towards the removal efficiency of heavy metals from aqueous solution using natural bentonite was reported by Kumar, et al. (2010). They found that the increase in the adsorbent dosage from 0 g to 1.2 g in one litre of adsorbate enhanced the fraction of zinc ion removed. The scenario occurred as a result of an increase in active sites provided by bentonite for more zinc ions to bind onto its surface. The argument provided by Kumar and co-workers (2010) was in agreement with the research done by Mishra and Patel (2009) with the use of

activated carbon, kaolin, blast furnace slag and fly ash have shown that maximum removal of zinc ions and lead ions were 20 g/L as beyond that, an exhaustion of actives sites took place.

The variation of temperature affects the entire thermodynamic system of the adsorption process. One of the notable studies which reflected such argument is by Sen and Khoo (2013) as they highlighted on the effect of increased temperature towards the adsorption capacity of zinc with three different temperatures of 30 °C, 50 °C and 70 °C. It was found that the adsorption capacity decreased with increase in temperature. Such result could be attributed to the decreased surface activity, indicating that the adsorption system exhibited exothermic process. The increase in temperature also weakened the force of attraction between clay adsorbent and zinc ions, causing a decrease in sorption activity.

The influence of contact time towards the adsorption capacity of the adsorbent is rather simple as also reported by Sen and Khoo (2013). There will be an equilibrium of the mass transfer of the metal ions between the solid surface and adsorbate up to a certain period of time. Every adsorbent possesses a distinctive equilibrium contact time due to different physical and chemical properties of the adsorbent. This has indirectly influencing the rate of uptake of the metal ions. They also found that the Zn-bentonite and Zn-kaolin system possess a similar equilibrium time at 80 minutes. The reason leading to such scenario is the similar physical and chemical properties of both materials itself.

The initial concentration of metal ions is the focus in this research to evaluate its effect towards the adsorption capacity of zinc. Salam, et al. (2011) and Thakur and Parmar (2013) reported on the effect of initial concentration on the adsorption efficiency for peanut husk charcoal and tea waste, respectively. The results indicated that the removal percentage decreased with the increase in zinc concentration from 10 mg/L, 20 mg/L, 40 mg/L, 60 mg/L, 80 mg/L up to 100 mg/L. The maximum removal of 60 % was achieved for 10 mg/L and this could be attributed to the exhaustion of the active sites on the adsorbent’s surface at higher zinc concentrations. Similar metal ions of interest with different adsorbent was used by Thakur and

Parmar (2013) to investigate the variation of initial concentration of metal ions at 10 mg/L, 20 mg/L, 50 mg/L and 100 mg/L using tea wastes. The fraction adsorption of zinc ions is independent of initial concentration at lower zinc concentration, causing the maximum removal percentage was 91 % at 10 mg/L. At higher concentration, number of heavy metal ions were higher compared to the availability of binding sites. A similar experiment was conducted for copper(II) and nickel(II) ions. They reported that the maximum removal of metal ions was attainable at 89 % and 94 %, respectively concluding that the amount of heavy metals uptake is dependent on initial metal ions concentration. The difference in percentage removal of metal ions was due to chemical affinity and ion exchange capacity.

A suitable adsorbent plays a crucial role as it determines the affinity of metal ions removal. The main requirements of adsorbent are high selectivity, capacity and long lifespan (Ruthven, 1984). With a higher capacity and longer lifespan, there will be more zinc being adsorbed and the adsorbent can be reused for a longer period of time. The focus of the research efforts in the past years concentrated on the use of various wastes to produce activated carbon. Bagasse, banana peel, carrot residues, castor seed hull, chestnut shell, coconut shell, palm kernel shell and tea are a few examples of agricultural wastes that have been studied in terms of zinc removal capacity shown in Table 2.3.

Those parameters need to be governed to achieve the best adsorption result prior to the subsequent processes. By doing so, there will be greater amount of zinc being desorbed in the later part of the experiment due to higher amount of zinc ions are loaded on the surface of the adsorbent.

Table 2.3: Adsorption capacities of different adsorbents in removal of zinc

Adsorbent	Adsorption capacity (mg/g)	Optimum conditions			Reference
		pH	Time (hour)	Temperature (°C)	
Bagasse fly ash	13.21	4	6-8	30	Gupta and Sharma, 2003
Banana peel	5.80	-	-	-	Annadurai, Juang and Lee, 2003
Carrot residues	29.61	-	1.1	-	Nasernejad, et al., 2005
Castor seed hull	6.72	5.8	-	-	Mohammod, et al., 2010
Chestnut shell (acid treated)	2.41	-	-	25	Vazquez, et al., 2009
Cocoa pod husk	100.95	-	2	-	Njoku, 2014
Coconut shell	9.43	-	0.8	-	Shrestha, et al., 2013
Coffee husk	5.56	5.4	-	-	Oliveira, et al., 2008
Mango peel	28.21	5	1	25	Iqbal, Saeed and Kalim, 2009
Palm Shell Activated Carbon	15.6	6	-	-	Issabayeva and Aroua, 2011
Risk husk ash	39.17	6	-	-	Akhtar, et al., 2010
Risk husk ash (Treated with H_2SO_4)	19.38	-	-	-	El-Shafey, 2010
Sawdust	6.93	5	-	-	Naiya, et al., 2009
Shell carbon (H_3PO_4 + Chitosan)	50.93	6	3	25	Amuda, Giwa and Bello, 2007
Tea waste	8.90	4.2	0.5	60	Wasewar, 2010
Wheat bran	16.40	6.5	24	-	Dupont, et al., 2005

2.3 Desorption of metal ions

The use of activated carbon is limited in that the metal ions are merely used to transfer onto the active sites of the activated carbon after adsorption; thus, it has indirectly posed another environmental issue, whereby the spent activated carbon is another potential waste. Therefore, in order to economize the adsorption process and adhere with the environmental regulation, the spent activated carbon can be reused through a proper regeneration step. There are few regeneration methods in the literature: thermal, chemical and biological regeneration (Gupta, et al., 2015). Chemical regeneration is performed using a specific solvent to desorb the heavy metals from the surface of adsorbent. A summary on various types of desorption medium used on different zinc-loaded adsorbents is shown in Table 2.4. It is evident that hydrochloric acid is the most frequently used desorbing medium to recover zinc ions. The valuable heavy metals contained within the desorption eluent can be recovered for other useful applications.

Table 2.4: Desorption of zinc ions using different solvents

Adsorbent	Desorption medium	Desorption (%)	Cycle for regeneration	Reference
Cassava treated with acid	0.1 M H_2SO_4	94	5	Horsfall, Arbia and Spiff, 2004
C.pentandra hulls	0.15 HCl	82	1	Madhava Rao, et al., 2007
Modified palm shell	0.1 M EDTA	99	3	Kushwaha and Sudhakar, 2013
	0.1 M HCl	87		
	0.1 M NH_3	92		
Phaseolus aureus hulls	0.15 M HCl	70.8	1	Rao, et al., 2009
Physic seed hull	0.1 M HCl	36	1	Mohammad, et al., 2010
Oil palm ash	0.05 M $NaNO_3$	90	1	Chu and Hashim, 2002
Rice husk ash	0.1 M HCl	24.51	1	El-Said, et al., 2011
	0.1 M HNO_3	27.28		
	0.1 M H_2SO_4	18.53		
	0.1 M CH_3COOH	12.46		
	H_2O	10.4		
Strychnos potatorum seeds	0.30 M HCl	93.58	1	Kumar, 2013

2.4 Evolution of electrochemical recovery of metals

In 1971, Fleischmann, Oldfield and Tennakoon (1971) studied the electrochemical removal of copper ions from dilute solutions using porous, fixed and flow through electrodes. The porous electrode was prepared using flakes of carbon and graphite. Porous electrode aims to provide high surface area to volume ratio for maximum mass transfer driving force for the copper ions to pass through. The outcome of the experiment showed that concentration of copper ions in the wastestream reduced to below 1 µg/ml from 667 µg/ml which was a great step forward in electrochemistry field for purification of industrial effluent.

Mohamed and Yap (2006) conducted a series of experiments to study the effect of gold recovery from simulated cyanide solutions using different cathode materials for instance, activated Reticulated Vitreous Carbon (RVC), activated porous graphite, porous graphite, copper plate and stainless steel plate. A polarization characteristics test was done to observe the kinetic of the cathode meaning a high activation overpotential leads to a slower kinetic. With smaller polarization and higher achieved current density, they have suggested that the activated RVC is the best in terms of performance compared to the other cathode materials. From the application side, activated RVC exhibited the highest deposition rate with approximately 100 % of gold was recovered in one hour with initial gold concentration of 500 ppm. Besides, it also offers the advantages of high chemical and electrochemical stability, high surface area to volume ratio of the electrode. The drawbacks are high operational cost and its brittle structure.

Hankin and Kelsall (2012) attempted to recover copper(II) ion from the gold ore wastewater containing cyanide, sulphur and copper compounds. They used the conventional 3-electrode electrochemical cell. A comparison was made between the gold ore processed wastewater with the copper cyanide synthetic solution prepared with copper cyanide, sodium cyanide and calcium hydroxide in a purified water. However, there was an autocatalytic reaction posed by the copper(II) oxide within the synthetic solution leading to a formation of thin layer of its metal oxide. This caused a rapid increase in current at a particular potential as compared to the gold ore

wastewater. This has enhanced the rate of removal of copper(II) ions from the wastewater through the autocatalytic reaction.

Colli and Bisang (2014) found that the concentration of the metal ions decreased from 100 ppm to 0.1 ppm within a few minutes. This was done by operating at low cell densities while maintaining a high cell output. They have made a comparison on the significance of the position of the counter electrode towards the behaviour of a cylindrical electrochemical reactor to enhance the effectiveness of the three dimensional electrode system. The arrangement of the three dimensional electrode with an outer counter electrode yields the best performance of the entire system having drained more current with the same potential difference a typical three dimensional electrode setup.

Qingwei, et al. (2014) examined several important parameters on the removal of cadmium in wastewater: initial concentration, initial pH, current density and complexing agents. The recovery ratio of cadmium metal can be maximized in acidic medium. When the current density was increased up to 4.46 mA/cm^2, the deposited mass of cadmium metal reached its maximum value. Besides, the recovery ratio of cadmium metal was affected in the presence of different complexing agents: sodium citrate, ethylenediaminetetraacetic acid (EDTA) and aqueous ammonia. The selection of the complexing agent affects the complex formation constant order. The use of aqueous ammonia has led to the highest recovery ratio of cadmium followed by the sodium citrate and EDTA.

2.5 Electrochemical deposition of metal

Electrochemical deposition of metal refers to the growth of a film through reduction of metal ions from aqueous, non-aqueous, organic and fused-salts type of electrolytes (Paunovic and Schlesinger, 2006). The type of electrolyte used in most of the studies is aqueous solution. The reduction of metal ions, M^{2+} is represented by a half equation of:

$$M^{z+}_{solution} + Ze \rightarrow M_{lattice} \quad (2.1)$$

The reduction step can be accomplished through a coupled processes: electrodeposition and an electroless deposition process. First, electrons are provided by an external power supply through electrodeposition step. A reducing agent in aqueous solution acts on electron source to trigger an electroless deposition process. Equation 2.1 illustrates a reaction between charged particles at solid-liquid interface. The potential difference across the interphase is a crucial parameter to be accounted. Another interphase is connected to the interface to form an electrochemical cell to measure potential difference.

When an electrode is introduced as an interphase where current is flowing across, its measured potential deviates from the equilibrium potential. The deviation is known as overpotential to overcome the hindrance posed by overall electrode reaction constituting a sequence of partial reactions. There are four rate controlling phenomena: charge transfer, diffusion, chemical reaction and crystallization (Gamburg and Zangari, 2011). However, most of the literature studies focused on diffusion controlled reaction for simplicity purpose. Diffusion controlled reaction involves mass transfer from bulk solution to interphase and vice versa.

The deposition of zinc on a known electrode surface occurs at potentials negative to the zinc reversible potential (Zhang, 1996). Normally, phenomenon of deposition of zinc is accompanied by hydrogen evolution at potentials negative to the zinc reversible potential. Hydrogen evolution is a more desired reaction at a cathodic potential owing to a more positive reversible potential. Ruetschi (1967) claimed that hydrogen evolution can be suppressed by reducing the solubilities of hydrogen in concentrated electrolyte. This can be done through the uses of sulphuric acid and potassium hydroxide as electrolyte to investigate the effect of electrolyte's concentration on solubility of hydrogen gas. Figure 2.1 shows an increase in the concentration of electrolyte reduces the solubility of hydrogen gas. This is due to salting out effect by ions with large hydration shell. Bockris, Nagy and Danjanovic (1972) proposed a method to ensure the cathodic reactions near the zinc reversible potential was dominated by deposition of zinc using aqueous solution of

concentration above 0.0001 M. This approach is also able to suppress hydrogen evolution.

$$2H^+ + 2e \rightarrow H_2\ (g) \qquad E_0 = 0.000\ V_{SHE} \tag{2.2}$$

$$Zn^+ + 2e \rightarrow Zn\ (s) \qquad E_0 = -\ 0.763\ V_{SHE} \tag{2.3}$$

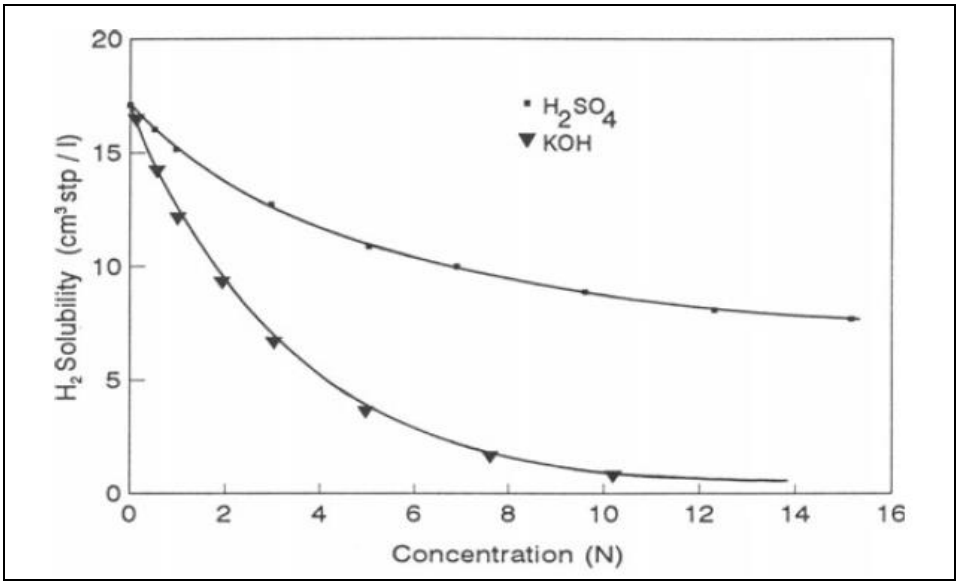

Figure 2.1: Solubility of hydrogen as a function of electrolyte's concentration (Zhang, 1996)

Apart from hydrogen evolution, oxygen reduction is another cathodic reaction affecting the electrodeposition of zinc. Oxygen reduction is a competing reaction similar to hydrogen evolution. The half equation for oxygen reduction in acidic solution is shown as:

$$O_2 + 4H^+ + 4e \rightarrow 2H_2O \qquad E_0 = 1.229\ V_{SHE} \tag{2.4}$$

While in alkaline solution is:

$$O_2 + 2H_2O + 4e \rightarrow 4OH^- \qquad E_0 = 0.401\ V_{SHE} \tag{2.5}$$

It is found that nitrogen gas is able to help in the reduction of amount of oxygen. The use of nitrogen gas to suppress reduction of oxygen was done by Pletcher, et al. (1991). They used an electrochemical cell with reticulated vitreous carbon (RVC) as cathode to treat an acidic sulphate solution. By doing this, the amount of copper ions in solution can be minimized. The concentration of copper ions was reduced 10 ppm to 0.1 ppm with overall efficiency of 84 % by flowing nitrogen gas continuously on top of sodium sulfate solution at pH 2 in batch process. Similar outcome was reported by Hatfield, Kleven and Pierce (1995) on the use of mine-drainage water to deposit copper metal. An encouraging outcome was shown as the initial concentration of 150 ppm decreased to less than 1 ppm with 99.9 % of copper recovered.

2.6 Electrochemical deposition parameters

In order to ensure a high efficiency of deposition of zinc on substrate's surface, Najafi, Shakeri and Ghasemi (2010) mentioned that parameters such as complexing agent, pH, concentration, current density and deposition time need to be optimized.

2.6.1 Complexing agent

Addition of complexing agents into bath solution contributes to the brightening of deposits, grain size reduction and enhancement of current density range. Kavitha, et al. (2006) investigated the use of different additives for instance carbonyls, thiosemicarbazide and thiosemicarbazone derivatives for the electrodeposition of zinc from sulphate baths. The bath were prepared within the acidic and alkaline range. Acetophenone (AcP), crotonaldehydethiosemicarbazone (CrTSCN), furfuraldehydethiosemicarbazone (FrTSCN) and salcylaldehyde (SaA) were used as additives. Table 2.5 depicts the outcome of the investigation and

furfuraldehydethiosemicarbazone proves to be the best additive in providing a reflective finishing of deposited zinc.

Table 2.5: Different additives in acid and alkaline electrodeposition baths (Kavitha, et al., 2006)

Additives	Acid bath			Alkaline bath		
	Concentration (mg/L)	**Nature of deposits**	**Current density range (A dm^{-2})**	**Concentration (mL/L)**	**Nature of deposits**	**Current density range (A dm^{-2})**
AcP	0.2	Dull	3.0-4.0	1.5	Grey	0.8-1.2
CrTSCN	1.5	Bright	1.0-3.0	1.5	Dull	1.0-2.5
FrTSCN	0.3	Mirror bright	0.2-8.0	1.5	Mirror bright	0.4-4.0
SaA	0.5	Semi bright	1.6-2.4	1.0	Satin white	0.4-1.2

Furfuraldehydethiosemicarbazone is the additive with the highest throwing power at 32 % and 48 % for acid and alkaline bath, correspondingly. Throwing power is defined as ability for metal to plate uniformly on electrode. Variation on the type of additive allows better suppressment of the side reaction at cathodic surface with a higher current efficiency. Kavitha, et al. (2006) used the same additives to determine the difference in terms of current efficiencies with respect to the one without any additive. Such investigation improved the current efficiency for furfuraldehydethiosemicarbazone from 85 % to 99 % in acid bath at current density of 2 Adm^{-2}. With similar setup and parameters of interest in alkaline medium, the current efficiency also improved from 91 % to 98 %.

Mo, et al. (2011) evaluated the use of sodium benzoate as additive on electrodeposition of zinc on carbon steel electrode from acidic chloride solution. The separation potentials were varied between -1.1 V_{SCE} to -0.6 V_{SCE}. The effect of sodium benzoate towards the formation and growth of zinc nuclei were notable in Figure 2.2 typically in terms of the blocking effect. By varying the concentration

sodium benzoate at 0 M, 0.007 M, 0.03 M and 0.04 M, the kinetics were different from one to another. One noticeable trend was when the additive's concentration was lower than 0.03 M, the rate of formation of zinc nuclei was accelerated and above 0.03 M, the additive would induce blocking effect towards the zinc electrodeposition. At a lower additive's concentration, formation and growth of zinc was favoured as a consequence of reduction of interface tension between electrode and solution. In the solution of higher concentration of benzoate, separation dominated causing retardation of the growth of zinc nuclei. Formation and growth of nuclei caused the one without benzoate, the deposited zinc in a big hexagonal crystal form whereas with benzoate, crystal size of electrodeposited zinc became smaller in size. Likewise, for orientation, at a lower concentration of benzoate, the deposited zinc in solution exhibits diffractions at crystal planes of (002), (100), (101), and (102), posing a characteristic structure of hexagonal crystal. The peaks were not viable at (002), (100), and (112) at the concentration of benzoate of 0.04 M due to the presence of amorphous structure of deposited zinc.

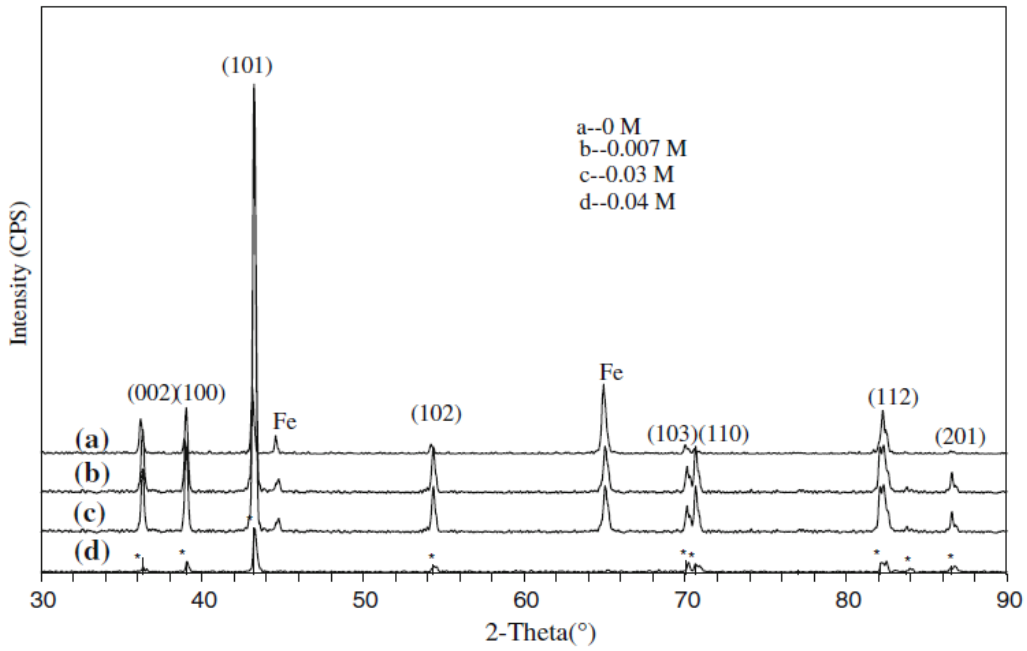

Figure 2.2: X-ray pattern of zinc deposited at different sodium benzoate's concentration (Mo, et al., 2011. p. 865)

2.6.2 pH

Electrolyte's pH has a significant influence on hydrogen evolution and precipitation of hydroxide. Hydrogen evolution results in hydrogen bubbles formation and convective effect near the electrode. Tuaweri, Adigio and Jombo (2013) reported that the increase in pH leads to an increase in cathodic current efficiency in the range of pH between 2.5 to 5. Below pH 4, current efficiencies were less than 100 %; whereas above pH 4, current efficiencies were beyond 100 % which was the desired outcome. Apart from the reason of excellent deposition conditions in the bath, another possibility could be the formation and subsequent co-deposition of zinc oxide and hydroxide. At higher pH values, the co-deposition of zinc oxide and hydroxide took place due to the occurrence of hydrogen evolution accompanied with an increase in pH near the cathode surface. Apart from current efficiency, it also causes morphological changes. The Scanning Electron Microscopy (SEM) micrographs in Figure 2.3 show the increase in pH causes the random orientations of zinc electrodeposits turned into a combination of lateral stacking sequence of zinc crystals and zinc platelets aligning almost perpendicular to the cathode surface.

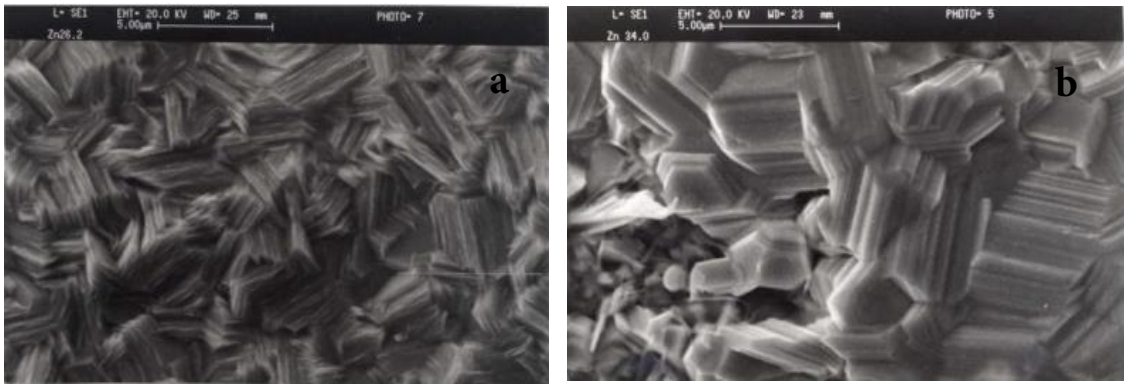

Figure 2.3: SEM Micrograph of zinc electrodeposit (a) pH 2.6 (b) pH 5 (Tuaweri, Adigio and Jombo, 2013. p. 22)

Bedir, et al. (2015) studied the effect of pH values on the electrodeposited Zn-Mn coating in a chloride-based acidic bath solution. The X-ray Powder Diffraction (XRD) patterns of the samples obtained in the solutions with different pH values is as shown in Figure 2.4. Basically, the phases of the electrodeposited Zn-Mn

alloy are dependent on the chemical composition of various co-precipitation pH values. With the increase of pH value, the XRD peaks of all samples were wider but peak widths decreased accordingly. Such result indicated that the average crystalline size for the deposited layers gradually increased with increase in pH value until 6, but not for the layer of pH 5. This is due to at pH 5, the peak intensities became weaker as a result of the dissolution of zinc hydroxide. By solely referring to the metal ion of interest, zinc from the Energy Dispersive X-Ray (EDX) result, it was found that the amount of zinc deposited was the least with 89.16 % at pH 5. This highlights that the dissolution of zinc is a huge factor towards the yield of zinc solid deposited. Thus, it provides an insight on the pH value should be used to obtain the greatest amount of zinc deposited within the constructed system in this research.

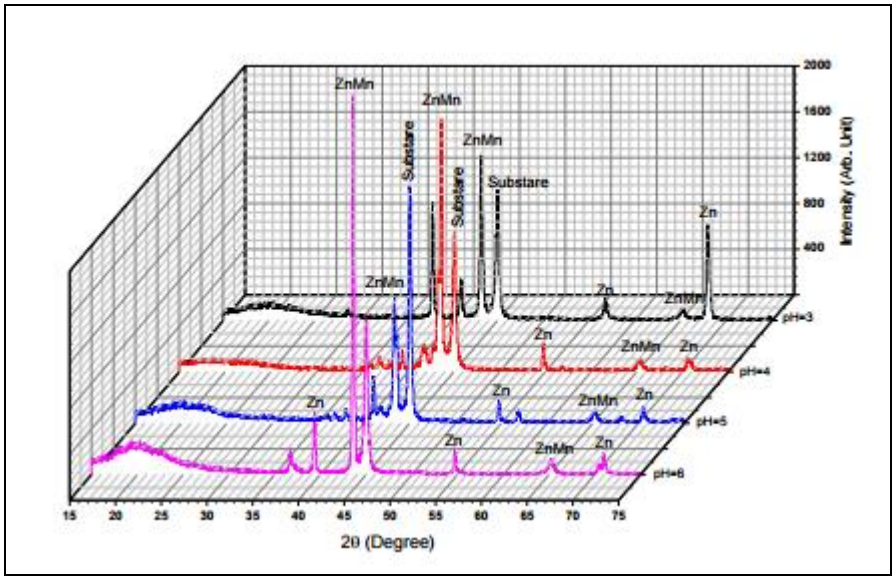

Figure 2.4: X-ray diffraction patterns of Zn-Mn alloy coatings with different pH values (Bedir, et al., 2015. p. 4516)

2.6.3 Concentration of electrolyte

The concentration of electrolyte affects the electrodeposition of metal. At ambient condition, the increase in concentration of metal ion increases the rate of metal deposition on the substrate. Krishnan, et al. (1996) evaluated the effect of

concentration on the electrodeposition of zinc from acetate bath in the range between 20 to 225 g/L using a system of Hull cell plate. At a lower concentration, 20 g/L, a powdery-like deposits were observed over a wide range of current density. With an increase of zinc acetate concentration up to 50 g/L, a powdery black deposits were in place of the previous greyish deposits with a higher range of current density due to better distribution of current. An improved current distribution leads to a better uniformity of the deposited zinc surface. Once the concentration increased to 125 g/L, a white film deposit was observed. At 175 g/L, negligible changes were observed on surface of deposit. This reflects on the effect of concentration of electrolyte in affecting the uniformity of the surface deposit.

Yao, et al. (2015) used an electrochemical approach to deposit ZnO with different electrolyte's concentration. They found that the average crystalline size of ZnO thin film depends on the electrolyte's concentration. The average crystalline size was 23.09 nm, 22.59 nm, 22.12 nm and 21.92 nm for 0.005 M, 0.01 M, 0.02 M and 0.03 M, respectively. The results could be attributed to the process of thin film growth are disturbed by the nucleus formation and crystal growth. With the increase of electrolyte concentration, the mass transfer of the liquid phase across cathode become faster leading to a high nucleation rate on the substrate. The higher nucleation rate causes more crystal nucleus on the cathode surface, thereby resists the crystal nucleus to grow larger due to lack of available space. Thus, when electrolyte concentration increases, the average crystalline size decreases.

The surface morphology of ZnO nanorods changes with change of electrolyte concentration as portrayed in Figure 2.5. At 0.005 M, some inclined and uneven nanorods were observed. The increase of electrolyte concentration has caused the density and inclination of ZnO nanorods increases as a result of ratio of non-polar planes increase on thin film surface. Also, the relative growth rate of non-polar planes decreased at higher electrolyte concentrations. This shows that surface morphology can be altered upon changes in electrolyte concentration.

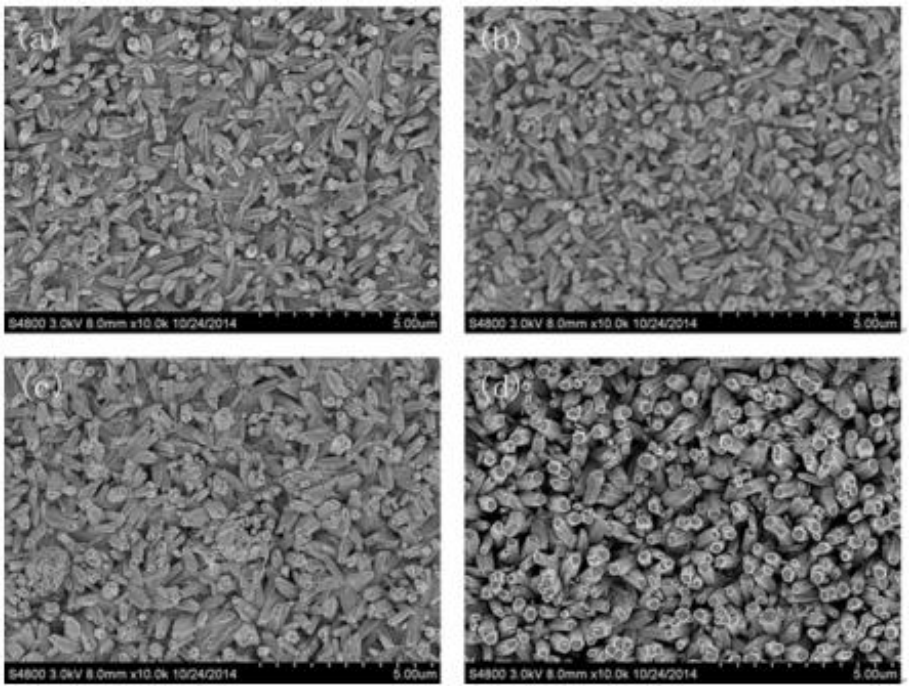

Figure 2.5: SEM micrographs of ZnO thin films in different electrolyte concentration: (a) 0.005 M, (b) 0.01 M, (c) 0.02 M and (d) 0.03 M (Yao, et al., 2015. p. 301)

2.6.4 Current density

Cathodic current density must remain constant within a proper range with respect to temperature and composition of bath. This ensures the uniformity of electrodeposit with a certain thickness. Low current density results to a poor coverage and low plating rate. Likewise, introducing excessive current is not essential with an increase rate of plating as it may liable to other difficulties. The effect can be portrayed in the presence of trace amount of impurities as this triggers the formation of dull electroplated surface (Gamburg and Zangari, 2011). An optimum range of current density for a given bath solution is dependent on its composition, operating condition and type of plating material.

Tuawei, Adigio and Jombo (2013) investigated the effect of current density on deposition process. With an objective to achieve a 8 µm thickness of zinc

electrodeposits, they examined a range of current densities of 2.0 – 5.0 A/dm^2 with pH 2.5 of bath solution as constant variable. At current density of 2 A/dm^2, 2.5 A/dm^2, 3.5 A/dm^2 and 4.0 A/dm^2, the time for deposition of zinc to achieve a thickness of 8 µm was 14 minutes, 11 minutes, 8 minutes and 7 minutes, respectively. At a lower current density, nucleation rate is low requiring a longer period of time for the layer of desired thickness of electrodeposit to ensure the full coverage of substrate. This reinforces an argument that an increase in current density is accompanied by a decrease in deposition rate. They also reported on the effect of variation of current density towards cathode current efficiency representing the contribution of side reaction on deposition of zinc. With a higher value of current density beyond 4.5 A/dm^2, hydrogen evolution as a side reaction dominated the entire reaction, allowing current efficiency to decrease notably. Thus, applied current density is a crucial parameter to be optimized which ensures minimum energy consumption.

2.6.5 Deposition time

In general, the thickness of electrodeposited metal increases with the deposition time. According to Faraday's law, amount of charges flowing in solution is in positive correlation with the flow of current and time. Popoola and Fayomi (2011) investigated the effect of deposition time towards zinc electrodeposition on low carbon steel substrates. It was observed that the weight gain increases with the increase of the plating time. However, the zinc ions do not deposit as continuous sheet from one edge of the cathode surface to another due to presence of discontinuities in the form of pores and cracks. With prolonged deposition time, the thickness of electrodeposit increases. Also, the stability of the process improved upon an even distribution of the grain structure on the cathode surface. Similar result is obtained by Tuawei, Adigio and Jombo (2013) with longer deposition time will be able to complement the reduced applied current density to achieve a certain thickness of electrodeposit.

CHAPTER 3

METHODOLOGY

3.1 Adsorbent

The commercially available palm shell based granular activated carbon (PSAC) was provided by Bravo Green Sdn Bhd, Malaysia. The PSAC with 8 × 30 mesh size and > 1100 iodine number was first sieved into the desired size of 850 µm to 1000 µm. The adsorbent was washed with deionized water (Milli-Q Millipore; 18.2 MΩ · cm resistivity) to remove fines. The wet adsorbent was dried in oven (Memmert® Universal Oven, Germany) at 110 °C for 6 hours. The prepared adsorbent was kept in desiccator for future use in the experiments.

3.2 Preparation of Stock Solution

All glassware was washed with detergent and rinsed thoroughly with deionized water, then soaked for 24 hours in 3 % of nitric acid (Fisher Scientific) and rinsed with deionized water. All chemicals were of analytical grade. 0.01 M of zinc nitrate hexahydrate, $Zn(NO_3)_2.6H_2O$ (Systerm, ChemPur) was prepared and used as stock solution to prepare solutions of different zinc concentrations.

3.3 Determination of zinc solution's pH

pH of zinc (II) precipitation is determined to prevent the formation of precipitate during the adsorption step (Chun-rong, et al., 2013). The solubility product constant for zinc hydroxide, K_{sp} is 6.8×10^{-17} at 25 °C (Haynes, 2014). In this computation, the initial Zn(II) concentration is 0.00015 M or 10 mg/L.

From the reversible dissociation equation:

$$Zn^{2+} + 2OH^- \longleftrightarrow Zn(OH)_2 \quad (3.1)$$

$$K_{sp} = [Zn^{2+}][OH^-]^2$$

$$6.8 \times 10^{-17} = [0.00015][x]^2$$

$$x = 6.7330 \times 10^{-7}$$

$$pOH = -\log [OH^-]$$

$$= -\log [6.7330 \times 10^{-7}]$$

$$= 6.172$$

$$pOH + pH = 14$$

$$pH = 14 - 6.172$$

$$pH = 7.828$$

The computation above shows that $Zn(NO_3)_2$ would be completely soluble in fairly acidic solution. Zinc hydroxide would precipitate at pH ≥ 7.828. Therefore, pH of the solution for adsorption must be maintained below pH 7.828 to enable maximum amount of zinc (II) ion to be adsorbed on the surface of PSAC. The pH of synthetic wastewater was adjusted through the addition of 0.1 M of sodium hydroxide or 0.1 M of hydrochloric acid solution. The pH of the synthetic wastewater was maintained at pH 5, a typical pH of industrial wastewater in Malaysia through a continuous monitoring using pH probe (Department of Environment, 2012). Regardless of 50 mg/L or 100 mg/L, this pH value will ensure minimal formation of precipitate prior to adsorption.

3.4 Preparation of Standard Solutions

Zinc standard solution (Fisher Scientific) of 1000 ppm was used for the preparation of the calibration standards. Seven calibration standards were prepared: 1 ppm, 2 ppm, 5 ppm, 10 ppm, 20 ppm, 50 ppm and 100 ppm by dilution method. Equation 3.2 was used to calculate the volume of deionized water needed. Calibration curve was plotted to establish functional relationship between zinc ions and the known concentration of it using Inductively Coupled Plasma Optical Emission Spectrometer (Optima 7000DV; Perkin Elmer). Deionized water was prepared as a blank solution to account for instrumental baseline.

$$M_1V_1 = M_2V_2 \tag{3.2}$$

where

M_1 = Concentration of analyte in standard solution (mg/L)
V_1 = Volume of the standard solution to be diluted (L)
M_2 = Final concentration of the solution after dilution (mg/L)
V_2 = Volume of the solution after dilution (L)

3.5 Adsorption experiments

The sorption of metals on palm shell activated carbon was studied using batch method. 5 g of granular palm shell activated carbon was immersed in a 100 mL of synthetic wastewater containing zinc and placed on a rotary shaker (Heavy Duty Rotary SH) at 180 rpm. The initial concentration of zinc solution was 10 mg/L. A contact time of one hour employed in the current research was more than sufficient to achieve adsorption equilibrium due to high adsorption tendency of the present PSAC. After a completion of batch adsorption step, the resulting solution was filtered using filter paper with pore size of 40 µm (Smith Scientific Limited). The concentration of the filtrate was measured using Inductively Coupled Plasma Optical Emission Spectrometer (ICP-OES) (Optima 7000DV; Perkin Elmer).

The amount of zinc adsorbed was determined by the difference between the initial and final concentrations of zinc in the samples. The percentage of removal of Zn^{2+} using palm shell activated carbon from prepared synthetic wastewater can be calculated using Equation 3.3.

$$\text{Percentage of removal of zinc ion} = \frac{C_o - C_t}{C_o} \times 100\ \% \qquad (3.3)$$

The experiment was repeated with a higher initial concentration of zinc solution, 50 mg/L and 100 mg/L to observe effect of initial concentration on adsorption capacity and electrodeposition efficiency.

3.6 Desorption experiments

Desorption experiments were conducted by using desorbing agents such as hydrochloric, nitric and citric acids. Two different concentrations were tested for each desorbing agent for evaluation of their effectiveness in stripping adsorbed zinc from the adsorbent's surface into the solution.

The zinc-loaded adsorbents from adsorption experiments were transferred into Erlenmeyer flasks which contained 100 mL of nitric acid solution (Fisher Scientific) of a specified concentrations, 0.1 M and 0.2 M. The selection of abovementioned concentrations were based on a study conducted by Hesas, et al. (2013). They used 0.1 M nitric acid to evaluate the desorption efficiencies of metal ions from rubber tire and coconut button. A great recovery of 98 % of nickel ions from the adsorbent was achieved. Thus, higher nitric acid concentration was used to observe effect of desorption efficiency.

The flasks were agitated on a rotary shaker (Heavy Duty Rotary SH) at 180 rpm for one hour at 25 °C. The resulting desorbing solutions were analysed for zinc content by using ICP-OES. Similarly, the experiments were repeated for hydrochloric acid, 0.1 M and 0.2 M concentrations. Since citric acid is a weak acid,

higher concentration is required. Therefore, 0.2 M and 0.5 M of citric acid were used. It was reasonable to select citric acid as desorbing agent due to similar type of weak acid was used by Bhatt and Shah (2013) on resin to desorb zinc ions at a concentration of 0.1 M, 0.5 M and 1.0 M. The research showed great results for concentrations of 0.1 M, 0.5 M and 1.0 M with desorption efficiencies of about 59.68 %, 62.73 % and 79.89 %, respectively were achieved.

The desorption efficiencies were computed in terms of the amount of zinc adsorbed during adsorption and stripped upon desorption as shown in Equation 3.4.

$$Desorption\ efficiency = \frac{Total\ amount\ of\ metal\ desorbed}{Total\ amount\ of\ metal\ loaded} \times 100\ \% \quad (3.4)$$

Apart from desorption efficiency, the volume of final desorbing solution is a critical parameter to be considered in this study. High volume of final desorption solution causes low concentration of zinc ions in solution. If the concentration of zinc ions in the solution is too low, there is a possibility of a zero recovery of zinc achieved in electrodeposition experiments.

3.7 Cyclic voltammetry test

3.7.1 Electrolyte preparation

Background electrolyte or supporting electrolyte was added into the working solutions from desorption step to enhance the flow of electric current and decrease energy consumption. Mehta and Sindal (2010) studied the use of different sodium salts as background electrolyte to minimize the occurrence of migration of zinc ions. The subject of interest was on the availability of other chemicals able to achieve the objective in a more effective way, for instance potassium salt. Calculation of the transport number to determine the suitability of either sodium or potassium salt used as supporting electrolyte was done. Potassium nitrate was found to be better in

suppressing the migration of electrons as compared to sodium nitrate. A factor of 100 to 1000 of concentration of supporting electrolyte as compared to concentration of ion of interest, Zn^{2+} was plausible. Therefore, a supporting electrolyte of 0.25 M potassium nitrate was added into the electrolyte to enable continuous current flow.

Besides, pH buffer was used to ensure a constant pH measurement so that the deposition conditions remained the same throughout the electrochemical reaction. Shaikh, et al. (2011) proposed the use of Britton-Robinson (BR) buffer in the electrodeposition of copper (II) ions onto graphite electrode at pH 1.63. The pH buffer solution was prepared by mixing 0.4 M of acetic acid, 0.4 M phosphoric acid along with 0.4 M of boric acid solution in proportionate volume ratio. In this research, pH buffer of pH 4 was prepared by titrating 0.2 M of sodium hydroxide into buffer solution. The pH buffer solution was added in 1:4 volume ratio to the potassium nitrate solution. The occurrence of hydrogen evolution and formation of hydroxides were minimized at optimal pH 4.

3.7.2 Electrode preparation

The platinum electrode needed to be lightly polished with alumina and rinsed with deionized water prior to each experiment. Surface of the graphite electrode was ground using fine-grain abrasive paper, polished with filter paper and rinsed with deionized water to provide clear reflective surface and a better reproducibility of the results. The tips of both electrodes were placed as close as possible at a distance of 0.2 cm to avoid significant ohmic drop between working electrode and reference electrode which may lead to incorrect potential measurement. The position of the reference tip should not interfere with the mass transfer of electrolyte species. All electrodes were static and remained in unstirred solutions during cyclic voltammetry.

3.7.3 Electroreduction behaviour of zinc

Cyclic Voltammetry (CV) experiments were conducted in a compartment of 100 mL glass cell at room temperature. Electrochemical reduction behaviour of zinc on stainless steel electrode in different electrolytes were performed using Autolab Metrohm potentiostat with NOVA 1.10 software. The final desorbing solution containing zinc and two aqueous solutions were sequentially prepared. One solution was desorbing solution composed of zinc and 0.25 M of potassium nitrate and another solution was upon addition of pH buffer as mentioned in the previous section.

A three-electrode electrochemical cell consisted of counter electrode, reference electrode and working electrode. Stainless steel electrode (area = 0.07 cm^2) was used as working electrode, the Ag/AgCl as a reference electrode and platinum wire (area = 0.1 cm^2) as counter electrode. Counter electrode acted as a sacrificial electrode to complete the circuit while reference electrode was to generate consistent potential within the electrochemical cell. The surface area of platinum electrode was ensured to be larger compared to the graphite working electrode to avoid the current limit at the working electrode by the counter electrode. The experimental setup is shown in Figure 3.1.

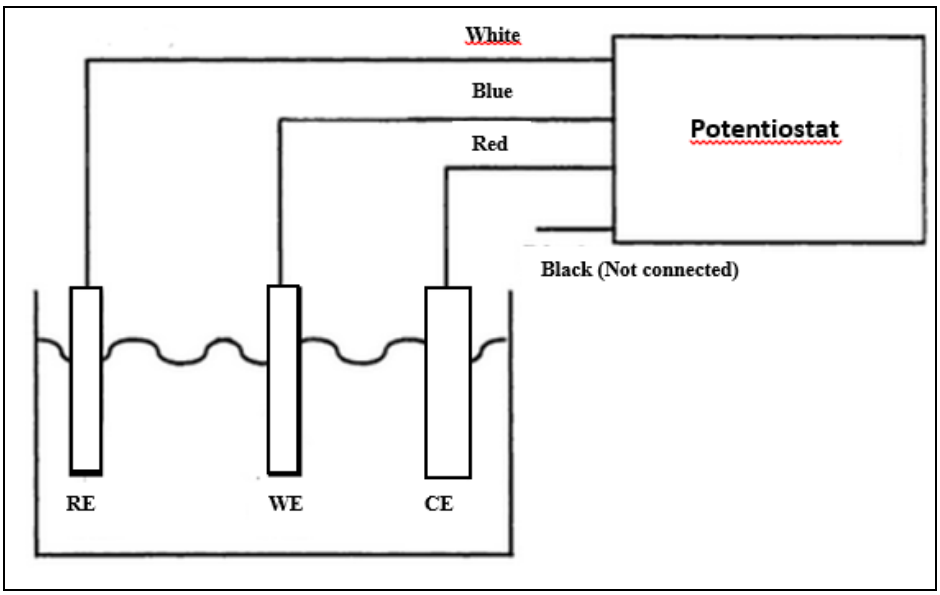

Figure 3.1: Three electrodes electrochemical cell setup

3.8 Zinc electrodeposition

For experiments on electrodeposition of zinc, a 200 mL electrochemical cell equipped with stainless steel cathode (area = 70 cm^2) and graphite anode (area = 0.1 cm^2) were used. The electrolyte was from resulting voltammetric experiments. The experiments were conducted with 100 A/m^2 applied current density, constant pH 4 at 25 °C. GW INSTEK Laboratory Direct Current (DC) Power Supply GPR-16H50D was used as source of DC current. The experiment was repeated with 200 A/m^2 applied current density for the best desorption agent. Similarly, deposition time of 10 and 30 minutes were tested.

The amount of zinc recovered was measured using ICP-OES and the percentage of zinc recovered was computed using Equation 3.5 shown below:

$$\text{Amount of Zinc recovered} = \frac{C_1 - C_2}{C_1} \times 100\ \% \qquad (3.5)$$

where

C_1 = Concentration of zinc ion before electrodeposition, mg/L

C_2 = Concentration of zinc ion after electrodeposition, mg/L

CHAPTER 4

RESULTS AND DISCUSSIONS

4.1 Adsorption of zinc on PSAC

Figure 4.1 illustrates the adsorption efficiency of zinc ions on PSAC as a function of initial metal ion concentration. The mean removal efficiency of zinc was 68.29 %, 95.35 % and 98.33 % for initial concentration at 10 ppm, 50 ppm and 100 ppm, respectively. The results showed that the amount of zinc adsorbed onto PSAC increased as the concentration of zinc ions increased; however, the difference for 50 and 100 ppm concentrations was slight.

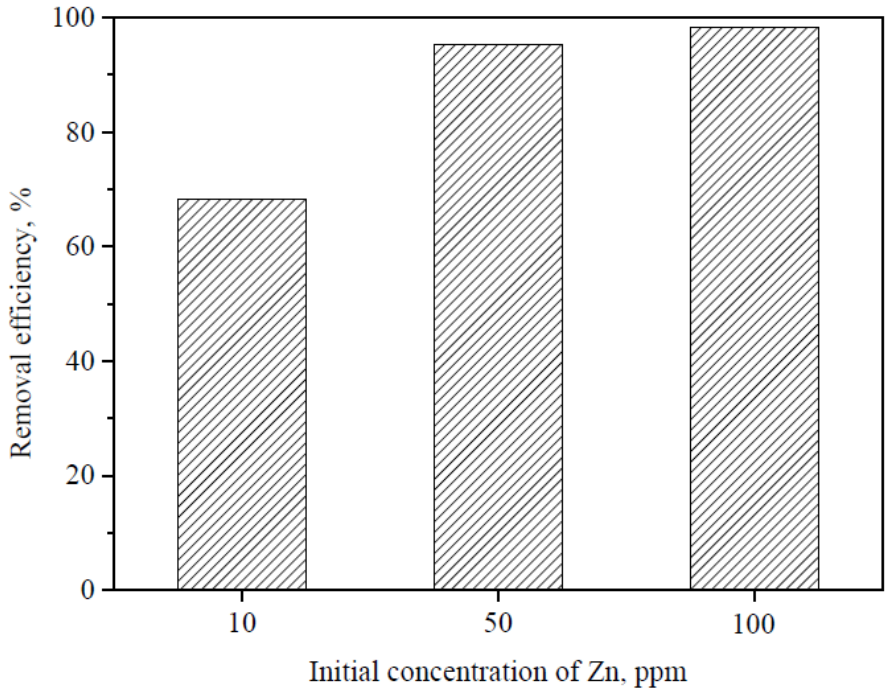

Figure 4.1: Removal efficiency for different initial concentration of zinc

At 10 ppm, low amount of zinc ions relative to the available number of adsorption sites caused the fractional adsorption to be independent of the initial concentration. Meanwhile at 50 ppm, removal of zinc indicated dependence on the initial concentration due to a higher driving force for mass transfer. However, beyond 50 ppm, the removal efficiency increased by a smaller margin of 3 % reaching maximum efficiency of 98 %. Insignificant increase of adsorption efficiency over increased concentration of zinc ions is probably associated with the exhaustion of the adsorption sites thus limiting adsorption of zinc ions from solution onto PSAC surface (Gupta and Sharma, 2003).

4.2 Desorption of zinc from PSAC

Three different type of acids were used for desorption of zinc into aqueous solutions.

4.2.1 Hydrochloric acid

Figure 4.2 depicts the desorption trend for hydrochloric acid as desorbing agent at different initial concentration of zinc. Two concentrations were tested to investigate the effects of concentration of desorbing agents on desorption efficiency. The result showed that recovery of zinc from adsorbent was favoured at lower concentration of acid. Such effect is probably caused by precipitation of zinc in a form of soluble salt of zinc chloride. Hydrochloric acid is dissociated into chloride ions and hydrogen ions forming metal chloride through proton-exchanging mechanism. Zinc can also form coordination complexes with chloride and hydroxide ions such as $Zn(OH)^{3-}$, $Zn(OH)_4^{2-}$, Zn_2OH^{3+}, $ZnCl^{+}$, $ZnCl^{3-}$, $ZnCl_4^{2-}$ and $ZnOH^{+}$ as modelled by chemical speciation software Visual MINTEG 3.1 (Gustafsson, 2014). Such metal complexes precipitated on the surface of adsorbent, typically at the narrow region of highly porous activated carbon preventing desorption of zinc ions into solution. Similarly, Booran, et al. (2015) reported recovery of about 87.3 %, 73.3 % and 67.4 % of Zn(II)

at concentration of hydrochloric acid of 0.1 M, 0.3 M and 0.5 M, respectively using continuous fixed bed system of wheat straw.

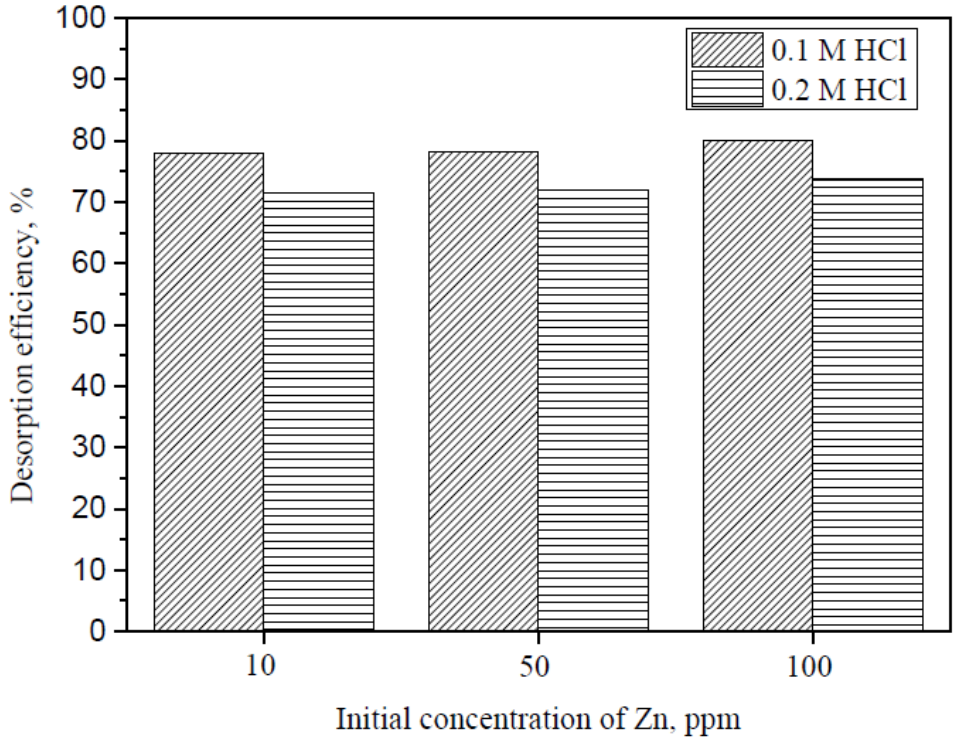

Figure 4.2: Desorption efficiency of zinc in 0.1 M and 0.2 M HCl

For 0.1 M HCl, desorption efficiency of 77.91 %, 78.25 % and 80.07 % was achieved for 10 ppm, 50 ppm and 100 ppm, respectively. The efficiency of desorption increased as the initial metal ions concentration in solution increased. PSAC exhibits a system containing predominantly micropores with a specific surface area of more than 1000 m^2/g (Chorkendorff and Niemantsverdriet, 2003). Metal complexes precipitated on the surface of PSAC, has restricted the access to adsorption sites, allowing the excess anions from the solution for instance, chloride ions adsorbed on the precipitate surface, again attracted Zn^{2+}. Adsorbed Zn^{2+} in turn adsorbed more anions and resulted in a multilayer adsorption. This contributed to the increase in loading from monolayer to multilayer adsorption of Zn(II) ions onto the surface of the PSAC (Bux, Swalaha and Kasan, 1995). Thus, Zn(II) ions can be easily desorbed off from the PSAC.

4.2.2 Nitric acid

Desorption efficiency of 63.74 %, 67.50 % and 72.79 % was achieved in 0.1 M of HNO_3; whereas in 0.2 M of HNO_3, the desorption efficiency was 69.39 %, 72.45 % and 75.00 % for 10 ppm, 50 ppm and 100 ppm, respectively. A similar trend as compared to HCl was observed, whereby the amount of zinc desorbed increased when the initial concentration of adsorbate increased. At higher acid concentration, the desorption efficiency increased which may be attributed to the formation of fewer complexes, compared to hydrochloric acid solution, between the zinc and hydroxide ions present in the solution. Visual MINTEG speciation profile indicated presence of the following complexes: $Zn(OH)^{3-}$, $Zn(OH)_4^{2-}$, $Zn_2(OH)^{3+}$, $ZnNO^{3+}$ and $ZnOH^{+}$. The desorption phenomenon observed in HNO_3 is probably mainly due to ion exchange interaction rather than chemical sorption as proposed by Ipeaiyeda and Tesi (2014).

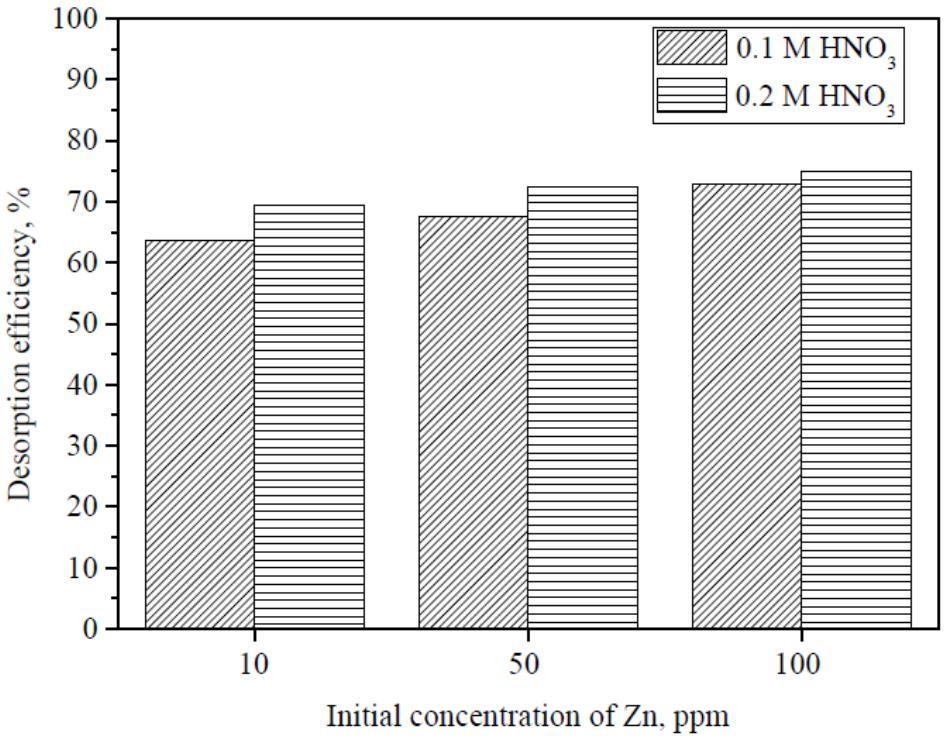

Figure 4.3: Desorption efficiency of zinc in 0.1 M and 0.2 M HNO_3

Comparison of desorption efficiencies between hydrochloric acid and nitric acid showed that hydrochloric acid is a better agent for desorption of zinc. Such

observation is linked to pK_a values of hydrochloric acid (-6.3) and nitric acid, (pK_a= -1.4), which is significantly smaller for the latter (Haynes, 2014). Thus, more protons will be liberated to exchange with zinc ions bound to the surface of PSAC using hydrochloric acid as compared to nitric acid (Rose and Devi, 2015).

4.2.3 Citric acid

Desorption efficiency of 61.90 %, 65.47 % and 71.66 % was achieved for 10 ppm, 50 ppm and 100 ppm, correspondingly, in 0.2 M of citric acid. However, in 0.5 M, the desorption efficiency decreased reaching 47.26 %, 56.39 % and 58.61 %, respectively. Figure 4.4 shows similar trend observed for hydrochloric and nitric acids: desorption efficiency increased as zinc ions concentration increased. As the concentration of acid used increased, the desorption efficiency decreased for all concentrations, similar to a trend observed for hydrochloric acid but different from nitric acid. A possible explanation is that a weak acidic condition provided by the citric acid solution at pH 3.51 promotes adsorption of Zn-citrate complexes instead of desorption of zinc ions as the acidic sites on the PSAC surface participate in the exchange of ions and complexes (Deepatana and Valix, 2004). The pH point of zero charge, pH_{pzc} is 9.25 from the characterization work done on PSAC by Chen (2013). This implies at pH 5, hydrogen ions residing on PSAC surface form positive surface charge. The adsorbed complexes are mainly $Zn(C_6H_5O_7)_2^{4-}$ and $Zn(C_6H_5O_7)^-$ in the solution as modelled by Visual MINTEG. The negatively charged complexes enhance the electrostatic interaction with the positively charged PSAC, thus promoting adsorption instead of desorption.

In contrast to both acids discussed above, citrate ions tend to form variety of complexes compared to chloride and nitrate ions. The desorption efficiency of citric acid was the lowest due to its small pK_a= 3.08 (Haynes, 2014). Among the three desorbing agents, hydrochloric acid appeared to be the most promising for desorption of zinc off PSAC surface into aqueous solution.

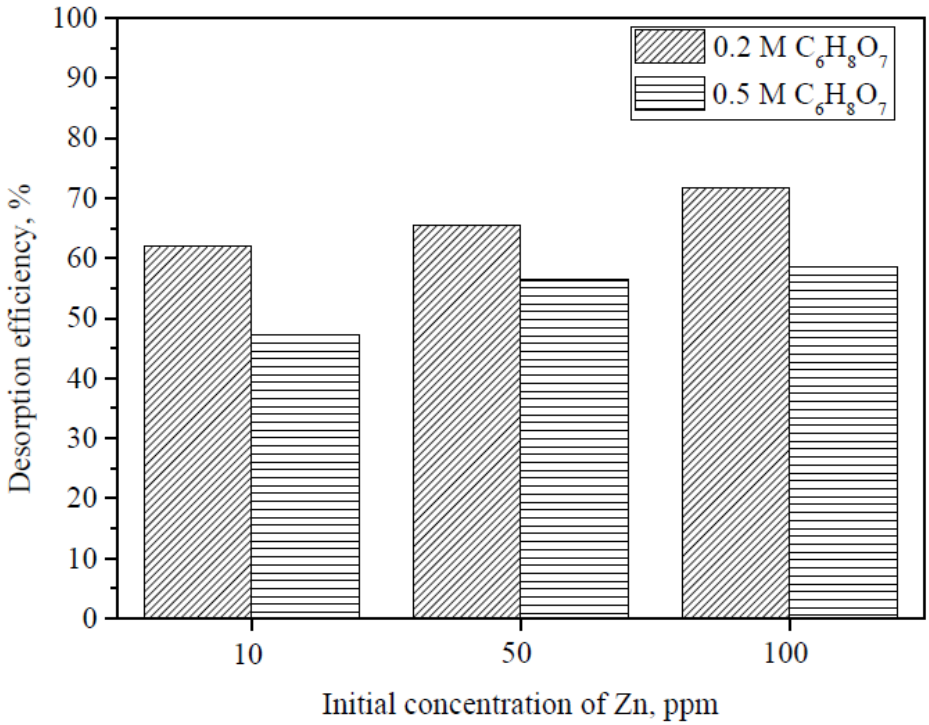

Figure 4.4: Desorption efficiency of zinc in 0.2 M and 0.5 M $C_6H_8O_7$

4.3 Cathodic reduction behaviour of zinc ions

4.3.1 Reduction of zinc in 0.1 M HCl

Prior to the electrodeposition study, the electro-reduction behaviour of zinc was studied using a cyclic voltammetry method on stainless steel electrode. In addition, potassium nitrate was used as supporting electrolyte and pH buffer was added to the aqueous solution. Figure 4.5 shows cyclic voltammogram for 10 ppm of Zn in 0.1 M HCl solution at a scan rate of 0.1 V/s. The potential scan was initiated in a negative direction from the open-circuit potential at 0 V. A range of different potentials were attempted to obtain the reduction peak for the first sample. However, no reduction peak was observed at any of the tested potentials even at the potential of -1.45 V. Thus, reduction peak was not detected in aqueous solution containing only zinc. The CVs for 0.1 M HCl solution shows forward and reverse scans. The forward scan indicates that the potential sweeps from 0.0 to −1.45 V while during the reverse scan, the potential sweeps back from −1.45 to 0.0 V. An anodic peak was observed at

around -0.10 V which reflects the anodic dissolution of the previously electrodeposited zinc metal. Since oxidation of zinc is beyond the scope of the research, therefore it will not be further discussed.

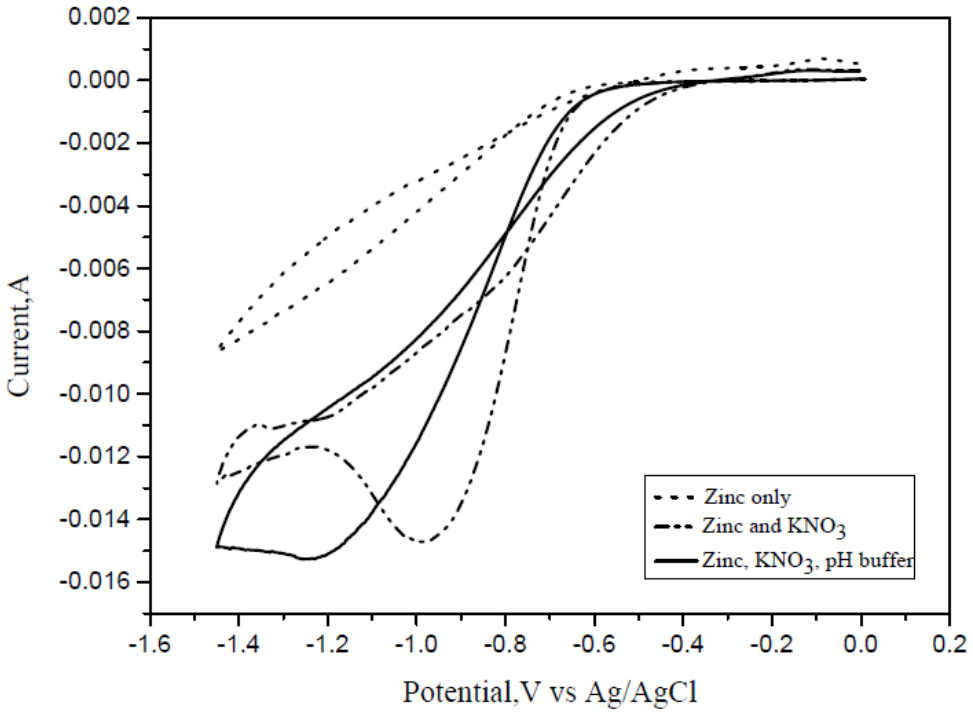

Figure 4.5: Cyclic voltammogram for 10 ppm of Zn in 0.1 M HCl

Resistance between the conductive ions was reduced when an inert background electrolyte was added. During forward scan, no current was observed until a potential of -0.5 V, which indicates reduction of Zn^{2+} into metallic Zn on the cathode. Beyond this potential, cathodic current increased as a result of zinc crystallization. The reverse potential was extended beyond -1.45 V in search for further reduction peaks. However, only one reduction peak was observed at a reduction potential of -0.98 V in the solution of zinc with supporting electrolyte. The observed peak was broad which is attributed to the occurrence of hydrogen evolution. The diminution in the current beyond the peak towards potential at 0.0 V can be explained by the decrease in the electrolyte concentration within the diffusion layer around the cathode surface. During the reverse scan, hydrogen reduction has slowed down significantly starting from the switching potential which resulted in gradual current drop. A crossover feature between forward and reverse scan was noticeable at

a potential of -0.80 V. which is characteristic for nucleation reaction (Ahmed, et al., 2013). However, no other distinctive peaks were observed throughout the reverse scan. The current decreased to the initial potential indicating the completion of the reaction for zinc deposition at the cathode. Noteworthy, the cathodic reduction of zinc was favoured by the addition of KNO_3 to the solution that increased electrolyte conductivity.

The standard half-cell potential of Zn(II) is -0.76 V and at the tested potentials, Zn(II) should deposit on the cathode more readily. However, this value neglects the activity coefficient of the ions. Figure 4.5 shows the deposition potential of zinc solution added with KNO_3 is slightly higher as compared to the standard potential. This is due to the reduction potential of zinc ions on a foreign substrate (stainless steel) is higher than the reduction potential on the cathode made of a similar metal due to a difference in crystallographic substrate-metal. Therefore, the deposition of zinc on stainless steel substrate commences at a potential more negative compared to redox potential of Zn/Zn^{2+}.

The addition of pH buffer containing biphthalate ions, $HC_8H_4O_4^-$ and potassium ions has shifted the deposition potential to more negative, -1.22 V. The peak is followed by a current plateau at about 15 mA beyond the peak during the forward scan indicating a mass transfer control of the process. One of the possible explanation for the increase in deposition potential is formation of variety of coordination complexes and molecules in aqueous solution such as $Zn(OH)^{3-}$, $Zn(OH)_4^{2-}$, $Zn(C_8H_4O_4)_2^{2-}$, $ZnCl^{3-}$ and $ZnCl_4^{2-}$ as modelled by chemical speciation software Visual MINTEG. The complexes consist of positively charged zinc ion surrounded by negatively charged anions with overall negative charge. The dissociation of abovementioned complexes is required to release zinc cations from the negatively charged ligand that in turn requires higher reduction potential due to the shift of the equilibrium potential to a more negative values through decreased activity of free ions (Gabe, 1978).

The cathodic peak current for an electrolyte solution with buffer was 15.26 mA, higher than that obtained without the addition of buffer, 14.72 mA. The increase in cathodic current is likely to be due to more reactions taking place involving

biphthalate, hydroxide and chloride ions. The addition of pH buffer is necessary to maintain pH of the electrolyte constant throughout the deposition process. During the voltammetric run, hydrogen evolution occurring at the cathode consumes the hydrogen ions from the electrolyte. This contributes to the release of hydrogen gas and causes increase in pH near the electrode surface. Therefore, the presence of the biphthalate ions buffer inhibits the precipitation of metal hydroxide as a result of the increase in pH value beyond 4. Apart from that, the amount of zinc deposited expressed in terms of yield is predicted to be the highest at pH 4 with the highest cathodic current efficiency of 98.8 %, reported by Abou-Krisha (2012) to deposit Zn-Ni-Fe alloys from a sulfate bath. Thus, the addition of pH buffer to the electrolyte promoted an increase of the resistivity and viscosity of the electrolyte and an increase of the reduction potential and the energy consumption.

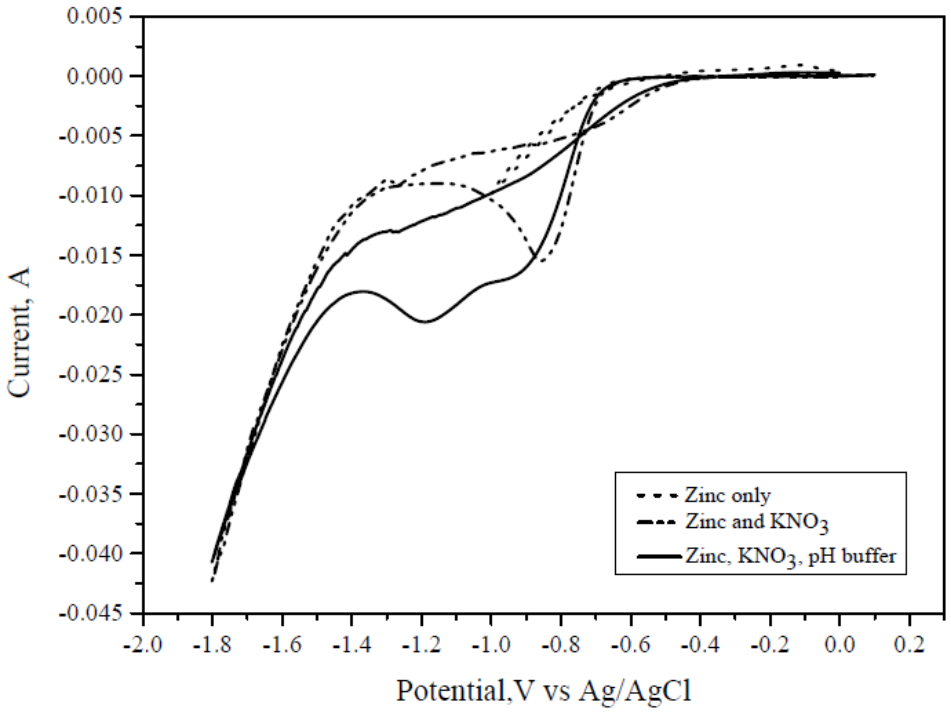

Figure 4.6: Cyclic voltammogram for 50 ppm of Zn in 0.1 M HCl

The electro-reduction behaviour of zinc in 0.1 M HCl at 50 ppm is presented in Figure 4.6. Even though the concentration of adsorbate was higher, all CVs exhibit similar features as discussed for Figure 4.5. No reduction peak was observed in electrolyte containing zinc only. Upon addition of KNO_3, a slightly

sharper reduction peak was notable at potential of -0.86 V as compared to the one in Figure 4.5. KNO_3 serves as conductivity salt allowing redox reaction occur more readily due to the presence of large number of dissociated ions accelerating electron transfer. At 50 ppm, the reduction potential was slightly less negative as compared to 10 ppm, -0.98 V. Such result is in accordance to the Nernst Equation: the higher concentration of Zn^{2+}, the lesser applied voltage is required. This is probably due to a decrease in the concentration overpotential meaning that the difference between the reduction potential voltage determined thermodynamically and experimental potential is decreased.

The addition of pH buffer increased the reduction potential to a more negative value at -1.19 V, caused by formation of coordination complexes requiring more energy to discharge Zn^{2+} ions. However, lower applied voltage is needed at higher concentration of zinc ions which can be justified by a less negative reduction potential at 50 ppm as compared to 10 ppm. A higher cathodic current at higher initial concentration was noticeable for every CVs in Figure 4.6 as compared to Figure 4.5 due to occurring zinc ions reduction further intensified due to higher amount of zinc ions present in the electrolyte.

Figure 4.7 shows the electro-reduction behaviour of zinc in 0.1 M HCl at 100 ppm. The reduction peak for solution containing zinc only was absent similar to the CVs in the previous two figures. Addition of KNO_3 caused the reduction peak to appear at -0.85 V and upon addition of pH buffer, the peak appeared at -0.97 V. Comparing initial concentrations of 100 ppm to 10 and 50 ppm zinc solutions, the required applied voltage was the lowest since the concentration of Zn^{2+} of the present electrolyte was the highest. However, the cathodic current decreased slightly as compared to 50 ppm due to phenomenon of hydrogen evolution was greatly suppressed at higher zinc concentration. Under such suppressing effect, only zinc reduction should be happening as less hydrogen gas bubbles were observed during the experiment. H^+ reduction would occur more favourably than Zn(II) reduction due to hydrogen's lower standard reduction potential requiring higher current. Another possible explanation is the shielding effect provided by zinc ions allowing greater occurrence of zinc reduction due to larger ionic radii covering the cathode surface. Ionic radius for hydrogen and zinc ions are 0.012 Å and 0.74 Å, respectively

(Barbalace, 2015). Sharma (2011) suggested that cathodic current increases exponentially with increasing hydrogen ions concentration. Another supportive argument is that a very sharp peak was observed in Figure 4.7 as compared to the previous figures for two CVs, (1) Zn + KNO_3 and (2) Zn + KNO_3 + pH buffer. This confirms that hydrogen reduction phenomenon was minimal in this case and zinc reduction dominated.

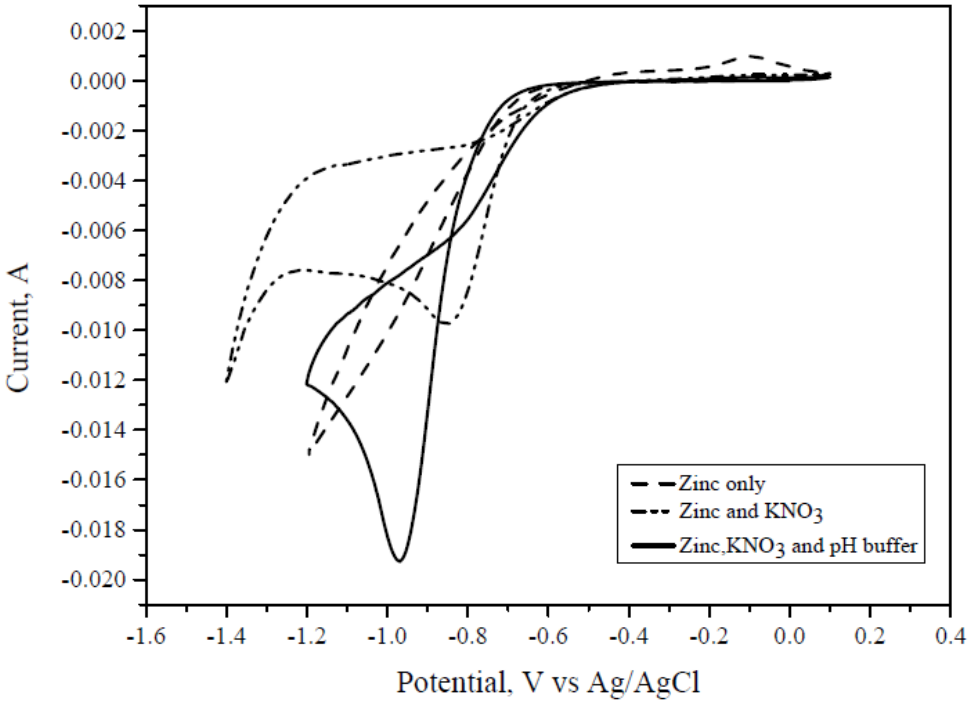

Figure 4.7: Cyclic voltammogram for 100 ppm of Zn in 0.1 M HCl

4.3.2 Reduction of zinc in 0.2 M HCl

Representative voltammogram of the electro-reduction behaviour of zinc in 0.2 M HCl at 10 ppm is portrayed in Figure 4.8. Even though the concentration of acid was increased to 0.2 M, the CVs exhibit a similar feature as discussed in Figure 4.5. Higher cathodic current was required, whereby hydrogen reduction occurs as a secondary cathodic reaction. The increase in acid concentration increased the concentration of hydrogen ions in the solution. Hydrogen evolution was further intensified due to higher concentration of hydrogen ions increasing the reaction rate

accordingly. This causes adsorption of hydrogen on stainless steel surface reducing the active area and enhancing the resistance between the bulk electrolyte and electrode. Hydrogen gas is produced through the combination of hydrogen atoms adsorbed on the electrode. Concurrently, an increase in hydrogen ions concentration caused the viscosity of electrolyte to increase slightly. Another difference in terms of CV is the influence of chloride ion towards the anodic potential. It was found that the anodic potential in the electrolyte increased from -0.01 V to -0.005 V which shows a similar trend observed by Panda (2013) on the effect of added chloride ions towards the deposition of cobalt.

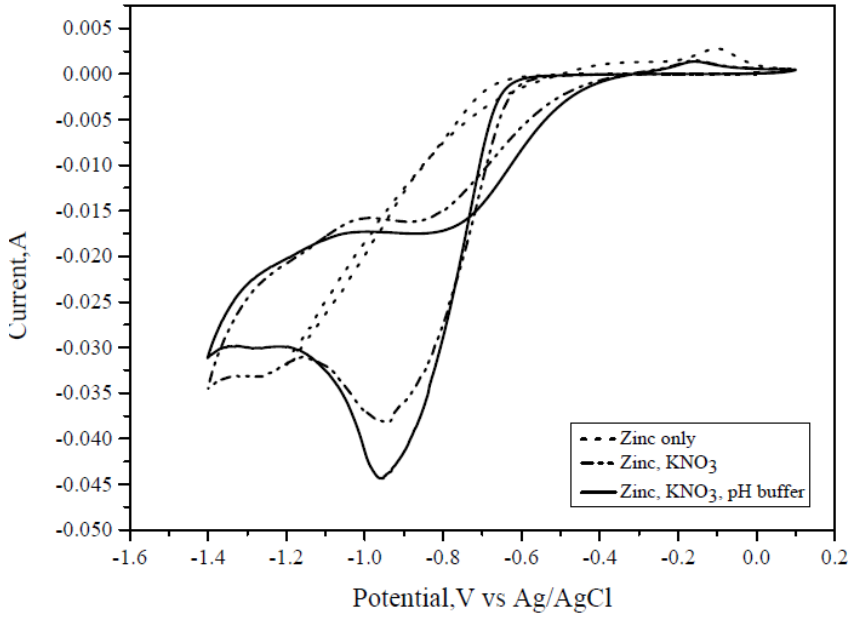

Figure 4.8: Cyclic voltammogram for 10 ppm of Zn in 0.2 M HCl

No reduction peak was observed in CV obtained from solution containing zinc only proving that conductivity of zinc ions is insufficient within the given time frame to carry out reduction. Once KNO_3 was added, peak appeared at a potential of -0.94 V with a peak current of 38.10 mA. Thus, KNO_3 is a suitable background electrolyte in two acid concentrations accommodating reduction of zinc. In comparison to the potential in Figure 4.5, reduction potential was reduced by 0.04 V under similar conditions but remained in the area of Zn^{2+} reduction. This happened due to ratio of hydrogen to zinc ions increased shifting to a less negative potential, in accord to Nernst equation. Horanyi (1996) and Ahmed, et al. (2013) demonstrated

that a strong adsorption of Cl^- caused a shift in reduction peak toward lower cathodic potential. In terms of cathodic peak current, it has nearly doubled from 14.72 mA indicating more reactions taking place, typically hydrogen evolution. The peak was broader as compared to the one in Figure 4.5 as the peak for electrodeposition of zinc is obscured by hydrogen reduction.

Addition of buffer agent lead to increase of the reduction potential up to -0.95 V with a peak current of 44.34 mA, significantly lower as compared to 0.1 M HCl at -1.22 V with peak current of 15.26 mA. These two reduction potential differences further reinforce the argument, thereby the increase in hydrogen ions concentration reduces the applied voltage. Panda (2013) suggested addition of chloride ions also reduces the cathodic voltage due to the readily discharge of Zn^{2+}-Cl^- complex at the cathode.

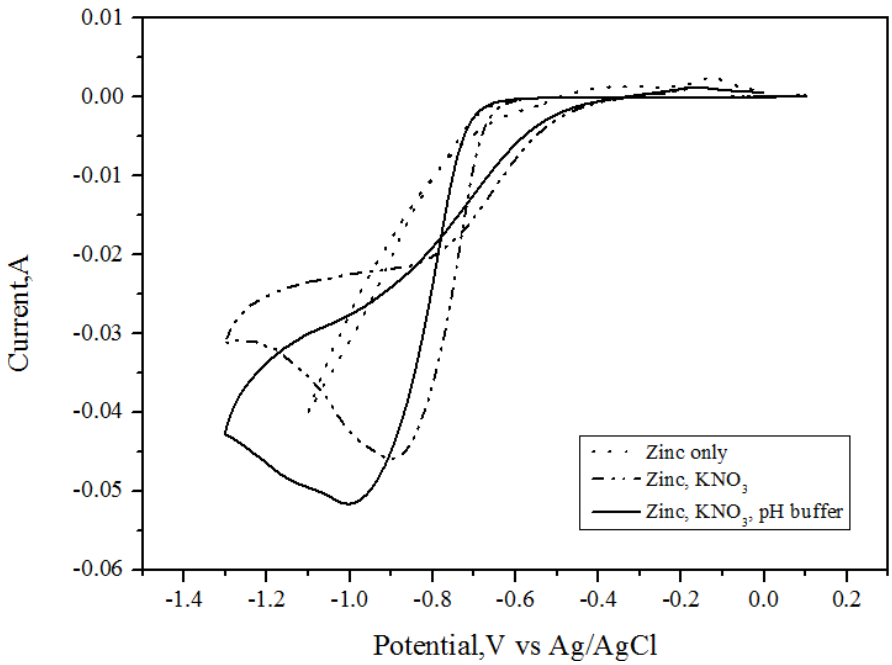

Figure 4.9: Cyclic voltammogram for 50 ppm of Zn in 0.2 M HCl

Similar trend was observed in Figure 4.9 as in Figure 4.6. Obvious difference is the cathodic current is slightly higher for every CV for instance, zinc solution containing KNO_3 is 45.89 mA. The applied voltage decreased from -0.98 V to -0.91 V and peak current increased from 15.78 mA showing a similar trend as discussed

for previous figures (Figure 4.5 and 4.8). The addition of buffer agent caused the peak potential to decrease to -1.00 V from -1.19 V upon the increased acid concentration to 0.2 M. The peak current also increased from 20.55 mA to 51.66 mA.

In Figure 4.10, similar findings as for Figure 4.9 were observed: (1) no reduction potential for solution with zinc only; (2) current required to carry out reaction decreased as a result of shielding effect in similar trend for 0.1 M HCl; (3) one reduction peak at more negative potential was observed upon addition of KNO_3; and (4) more reactions are taking place as buffer agent was added.

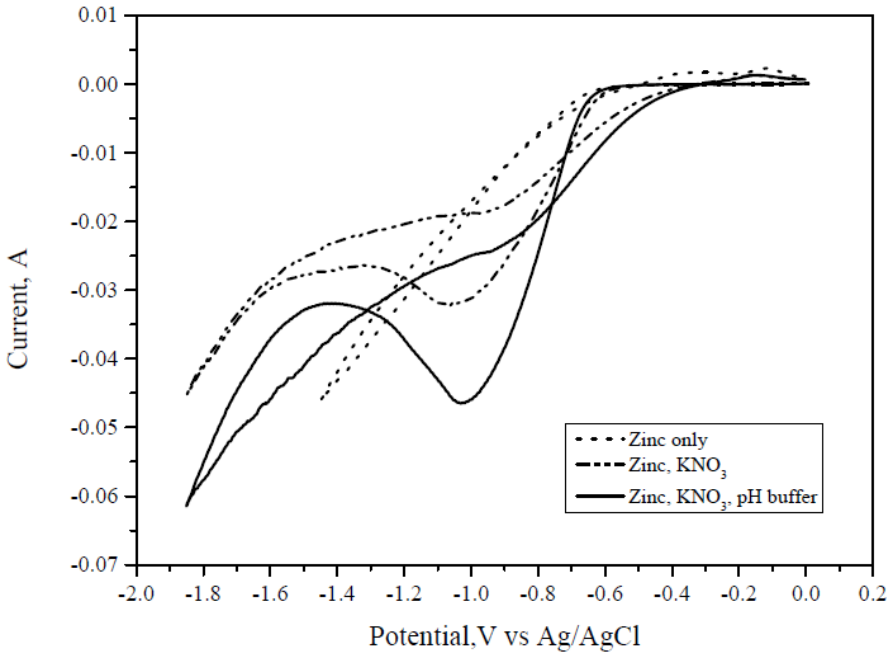

Figure 4.10: Cyclic voltammogram for 100 ppm of Zn in 0.2 M HCl

4.3.3 Reduction of zinc in 0.1 M HNO_3

Figure 4.11 shows the CV for 10 ppm of zinc solution in 0.1 M of HNO_3. Over the tested potential range, no reduction peak was observed in zinc only solution, similar to observation for HCl at the same concentration. Cathodic peak potentials of -0.87 V and -1.05 V were observed in zinc solutions with KNO_3 and buffer agent,

respectively. Cathodic peak potential shifted toward lower potential value when the desorbing agent changed from HCl to HNO_3 in the presence of supporting electrolyte. Ahmed, et al. (2013) related such changes to a higher blocking effect caused by chloride ions as compared to nitrate ions. The peak potential value was close to the reduction potential of nitrate ions of around -0.85 V vs Ag/AgCl (Manzano, et al., 2011). This has justified the presence of nitrate ions in the electrolyte. Cathodic reduction of Zn^{2+} is clearly improved in the presence of KNO_3.

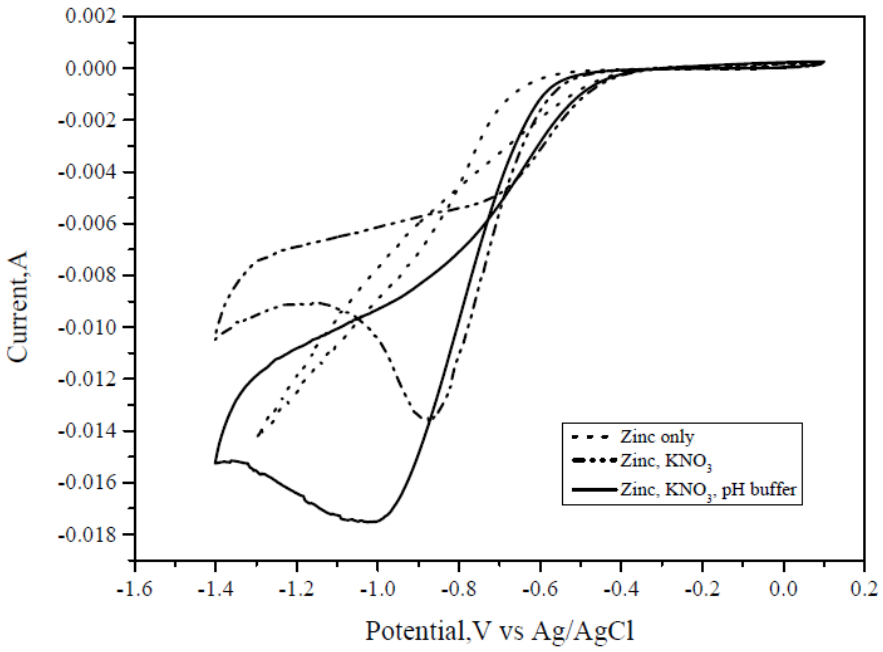

Figure 4.11: Cyclic voltammogram for 10 ppm of Zn in 0.1 M HNO_3

Upon addition of pH buffer, the peak current of broader shape reached 17.53 mA, higher than for 0.1 M HCl, 15.26 mA. The increase in cathodic current in the presence of buffer agent indicates that Zn^{2+} electroreduction is also favoured under present condition. However, the peak potential shifted to more negative potential due to formation of coordination complexes such as: $Zn(OH)^{3-}$, $Zn(OH)_4^{2-}$ and $Zn(C_8H_4O_4)_2^{2-}$ as visualized by Visual MINTEG. Higher reduction potential is needed to release positively charged zinc ions from ligands due to decline in activity of free moving ions. Comparison of two acids indicated that reduction potential under presence of buffer agent is lower for HNO_3 (From -1.22 to 1.05 V). This is

probably due to a fewer complexes formed in nitrate system as compared to chloride system.

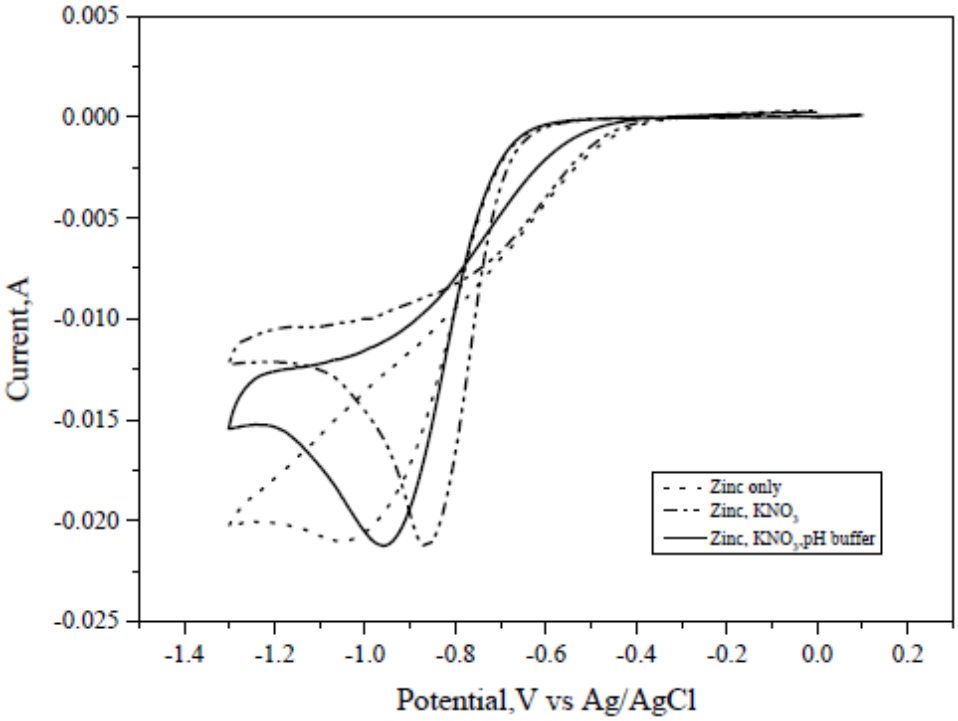

Figure 4.12: Cyclic voltammogram for 50 ppm of Zn in 0.1 M HNO_3

At 50 ppm, a distinct broad peak was observed in solution containing zinc only, in contrast to all above mentioned CVs proving that reduction of zinc occurs and concentration of zinc ions is critical factor. Conversely, higher reduction potentials for both CVs in the presence of KNO_3 and buffer agent in zinc solution as compared to HCl were achieved. Yoshida, et al. (2004) claimed that Zn^{2+} serves as a catalyst in reducing NO_3^- ions. At 10 ppm, the catalytic effect on NO_3^- ions reduction is negligible, whereas at 50 ppm, higher reduction of NO_3^- ions leads to the potential shift towards more negative value, typically beyond -1.0 V upon addition of buffer agent. Such finding could be attributed to the reduction of nitrate to nitrite ions which occurs at the potential close to -0.85 V vs Ag/AgCl. Meanwhile, cathodic current at 50 ppm was higher than in the CVs for 10 ppm indicating higher Zn^{2+} concentration promotes reduction of nitrate and zinc ions.

Similar trend can be observed in Figure 4.13 as compared to 50 ppm upon increased Zn^{2+} concentration. A sharper peak was observed for the solution containing Zn^{2+} only due to higher Zn^{2+}/H^{+} ratio limiting hydrogen reduction. The higher ratio gives a greater catalytic effect to reduce nitrate ions, requiring similar potential as in 50 ppm. Besides, higher cathodic current was needed compared to lower concentrations to carry out the reduction reactions.

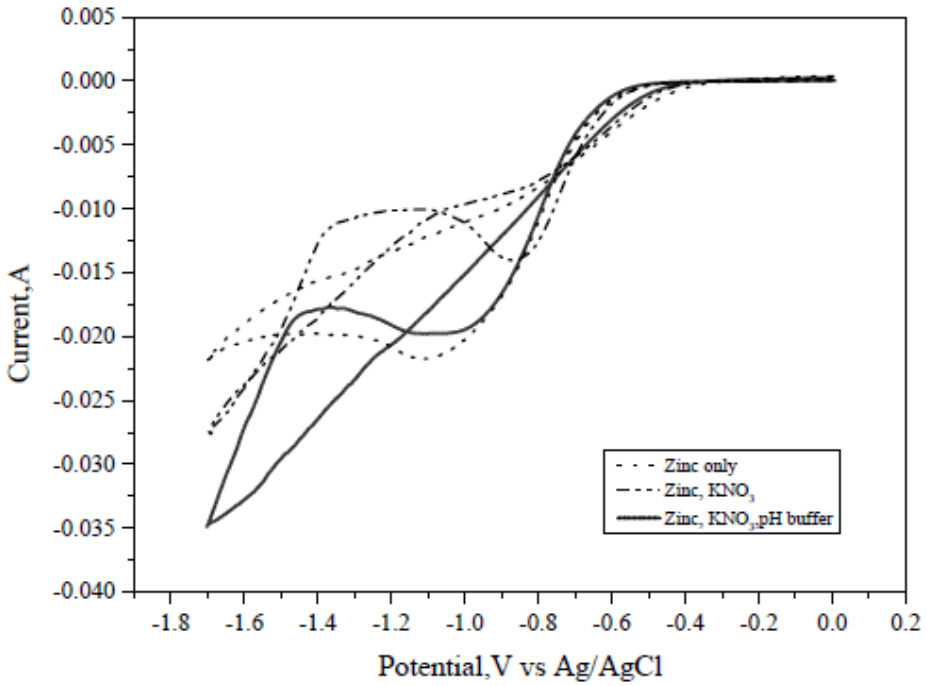

Figure 4.13: Cyclic voltammogram for 100 ppm of Zn in 0.1 M HNO_3

4.3.4 Reduction of zinc in 0.2 M HNO_3

Comparison of Figure 4.11 and 4.14 shows that increase in nitrate concentration caused a shift in reduction peak to lower cathodic potential for solutions with KNO_3 (From -0.87 to -0.85 V) and buffer agent (From -1.05 to -0.87 V). Besides, cathodic reduction of nitrate to nitrite ions also occurred at a less negative potentials suppressing zinc ions reduction. The process is diffusion controlled, whereby the voltammograms for Figure 4.11 and 4.14 depict in almost the same shape. In nitrate electrolyte, the limiting current for Zn^{2+} deposition increased with increasing nitric acid concentration as a result of Zn^{2+} diffusion. Gurevich (1989) suggested that the

influence of NO_3^- ions occurring in parallel with zinc ions reduction is the special feature of this system. Besides, the peak appeared to be sharper due to nitrate reduction has suppressed hydrogen reduction.

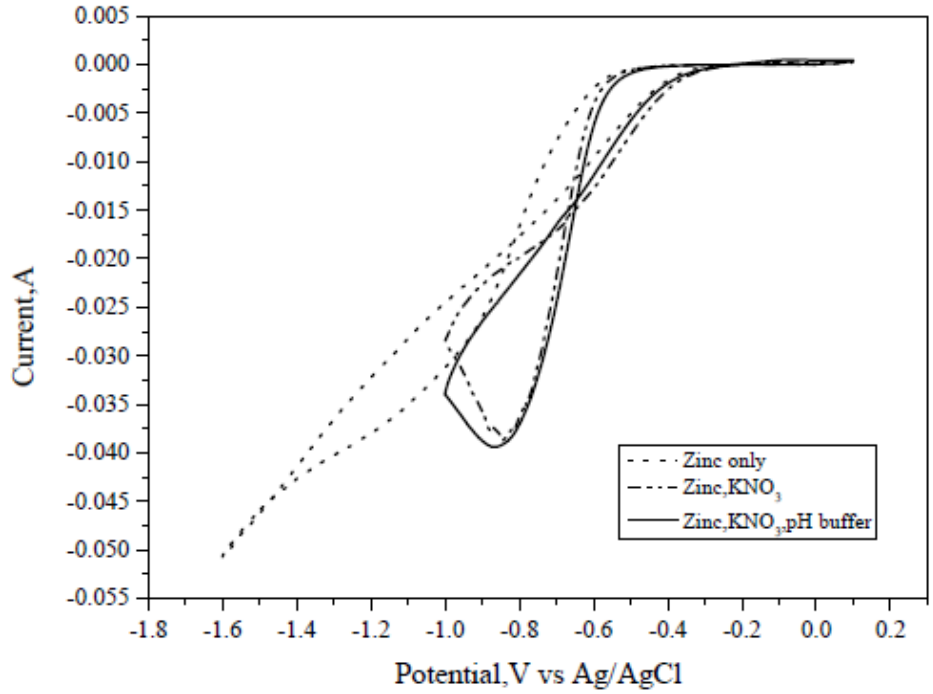

Figure 4.14: Cyclic voltammogram for 10 ppm of Zn in 0.2 M HNO_3

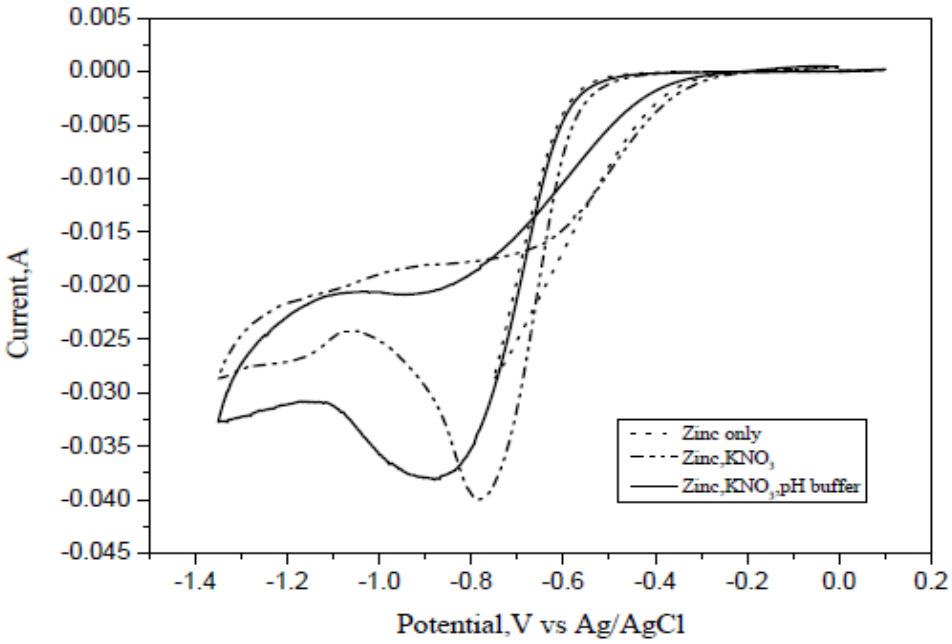

Figure 4.15: Cyclic voltammogram for 50 ppm of Zn in 0.2 M HNO_3

Figure 4.15 shows that the cathodic current slightly increased as compared to 10 ppm. The peak appeared earlier for higher concentration of Zn^{2+}, 50 ppm, when it acted as catalyst promoting electroreduction of nitrate species. Moreover, such effect also lead to a slight increase in peak potential in zinc solution with KNO_3.

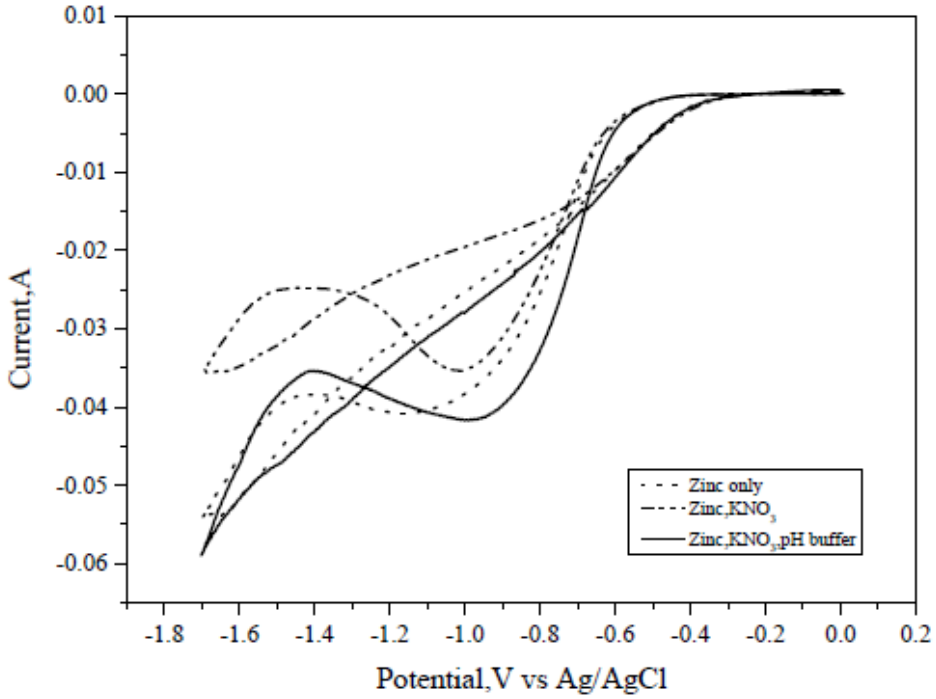

Figure 4.16: Cyclic voltammogram for 100 ppm of Zn in 0.2 M HNO_3

Similar trends can be observed in Figure 4.16: (1) reduction peak remained in CV for solution containing zinc only; (2) reduction potential of both zinc solution with KNO_3 and upon addition of buffer agent increased to a more negative potential; (3) higher cathodic current proving that more reactions taking place.

4.3.5 Reduction of zinc in 0.2 M $C_6H_8O_7$

Figure 4.17 shows the CV for the 10 ppm zinc solution in 0.2 M of citric acid. By contrast, it shows a very different behaviour as compared to hydrochloric and nitric acids. No reduction peak was depicted in solution containing zinc only and upon

addition of KNO_3 and buffer agents. There are several possible explanations for such results: (1) the reduction peak potential and hydrogen evolution happen at the same region and therefore cannot be separated; and (2) KNO_3 is not a suitable supporting electrolyte in the presence of citrate ions. These arguments are based on the observed alternating capacitive current without a clear reduction peak. Despite the absence of reduction peaks, slight increase in cathodic current was detected following the addition of KNO_3. Also, some effect upon the addition of pH buffer in terms of the voltammetric behaviour was noted. A possible explanation for this may be weak supporting electrolyte and buffer are adsorbed on the cathode surface through hydrogen bridge bonds. These adsorbed species on working electrode hinders the access of Zn^{2+} ions to the active surface of stainless steel electrode (Li, et al., 2007). Species present in the solution under such conditions include $Zn(C_6H_5O_7)_2^{4-}$, $Zn(OH)^{3-}$, $Zn(OH)_4^{2-}$, $Zn(C_8H_4O_4)_2^{2}$, $Zn(C_6H_5O_7)^{-}$ and Zn_2OH_3 as simulated by Visual MINTEG.

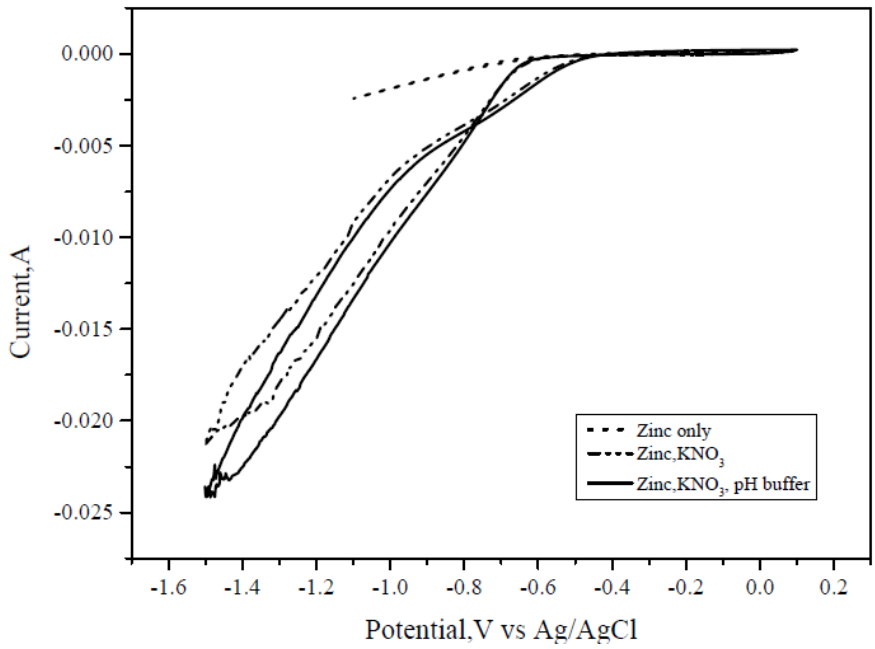

Figure 4.17: Cyclic voltammogram for 10 ppm of Zn in 0.2 M $C_6H_8O_7$

Increasing Zn^{2+} concentration to 50 ppm changed the cathodic potential to a less negative values which could be attributed to the decrease in concentration overpotential. It is also facilitated the nucleation of Zn^{2+} ions on the cathode. Higher cathodic current also signifies that the reduction phenomenon is favoured upon

increased Zn^{2+} concentration. However, no reduction peak was observed in any of zinc solutions, observation similar to 10 ppm solution discussed above.

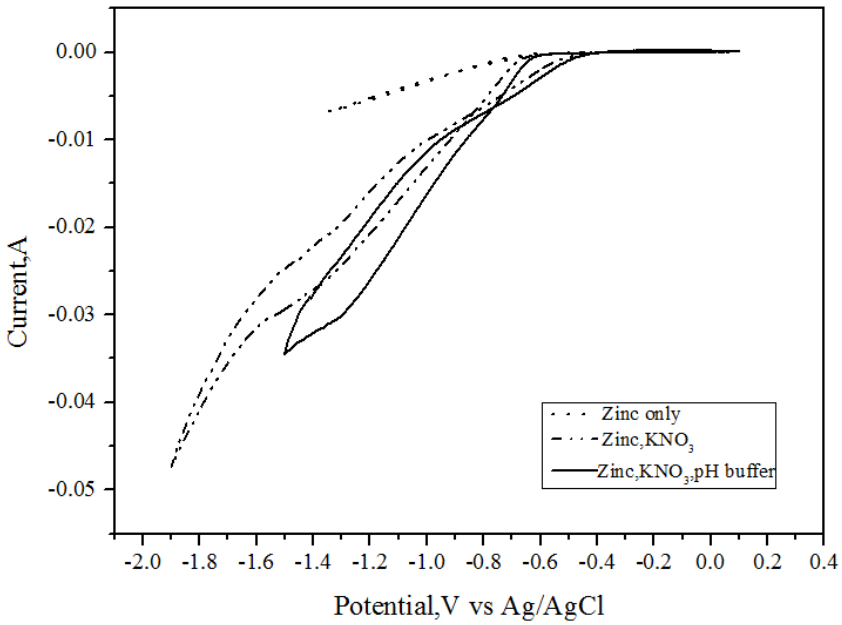

Figure 4.18: Cyclic voltammogram for 50 ppm of Zn in 0.2 M $C_6H_8O_7$

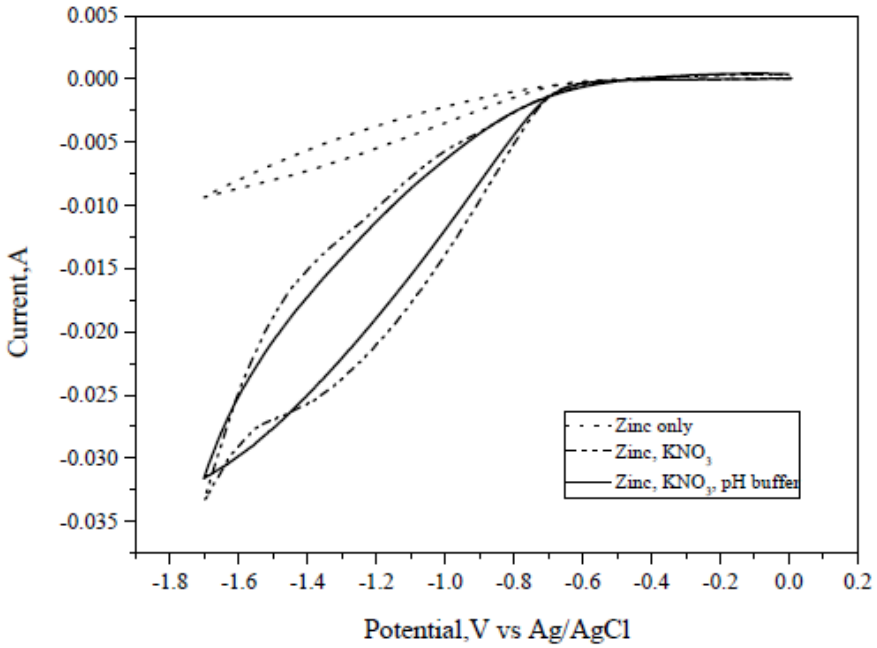

Figure 4.19: Cyclic voltammogram for 100 ppm of Zn in 0.2 M $C_6H_8O_7$

Figure 4.19 depicts similar CV as compared to Figure 4.18 despite doubled Zn^{2+} concentration. This shows that increasing concentration of metal ions beyond 50 ppm has a negligible effect in terms of cathodic current and potential. This means the amount of Zn^{2+} in the solution needs to have higher increment, more than double in order to alter metal ions' voltammetric behaviour from 50 ppm. This is probably due to the amount of Zn^{2+} complexes formed with citrate ions that inhibited electroreduction process at the cathode surface.

4.3.6 Reduction of zinc in 0.5 M $C_6H_8O_7$

The effect of increased concentration of citrate ions (0.5 M) can be observed referring to Figures 4.20 and 4.17. No reduction peak was detected within the tested potential range as in 0.2 M citric acid solution. The total citrate concentration was much higher than Zn^{2+} concentration meaning negligible amount of free Zn^{2+} ions are present in the solution thus electroreduction reactions are limited. The inhibition effect of citrate ions is likely due to formation of complexes blocking active sites on the cathode surface. However, a very slight increment in cathodic current contributed to the presence of hydrogen ions was noted.

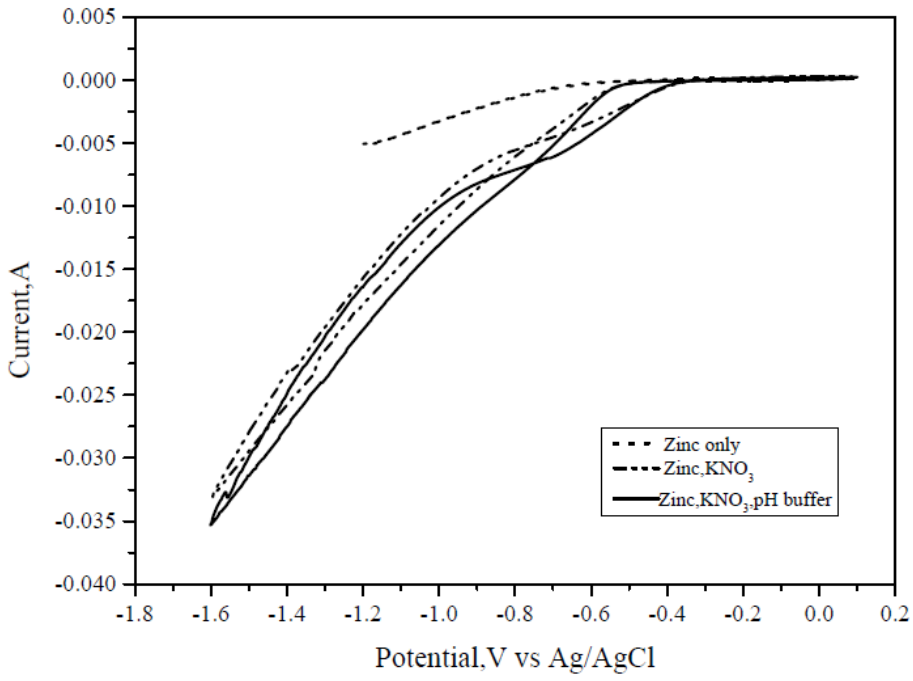

Figure 4.20: Cyclic voltammogram for 10 ppm of Zn in 0.5 M $C_6H_8O_7$

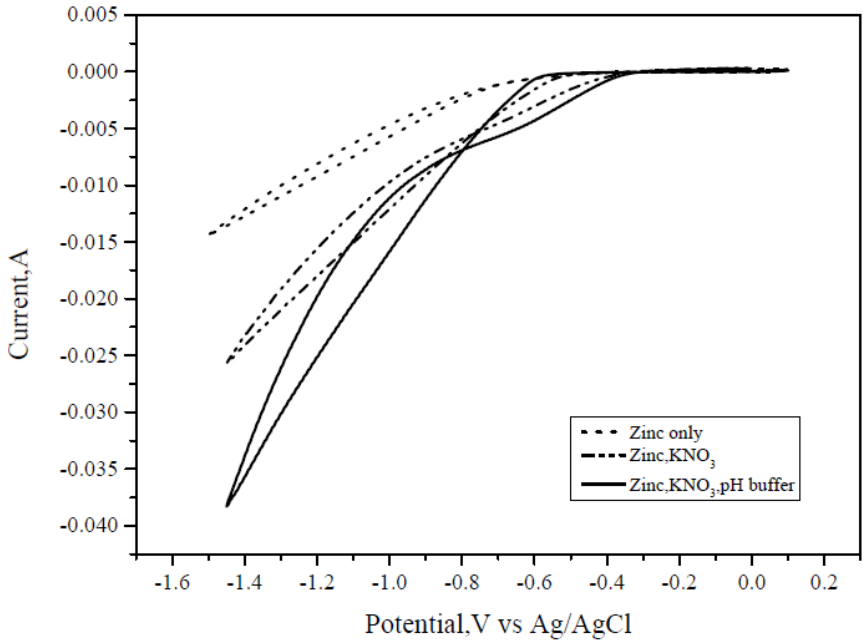

Figure 4.21: Cyclic voltammogram for 50 ppm of Zn in 0.5 M $C_6H_8O_7$

Figure 4.21 shows more significant differences in CVs for solutions containing Zn only, KNO_3 and buffer agent. Thus, addition of KNO_3 increased the cathodic current signifying the importance of conductive species presence to minimize migration effect.

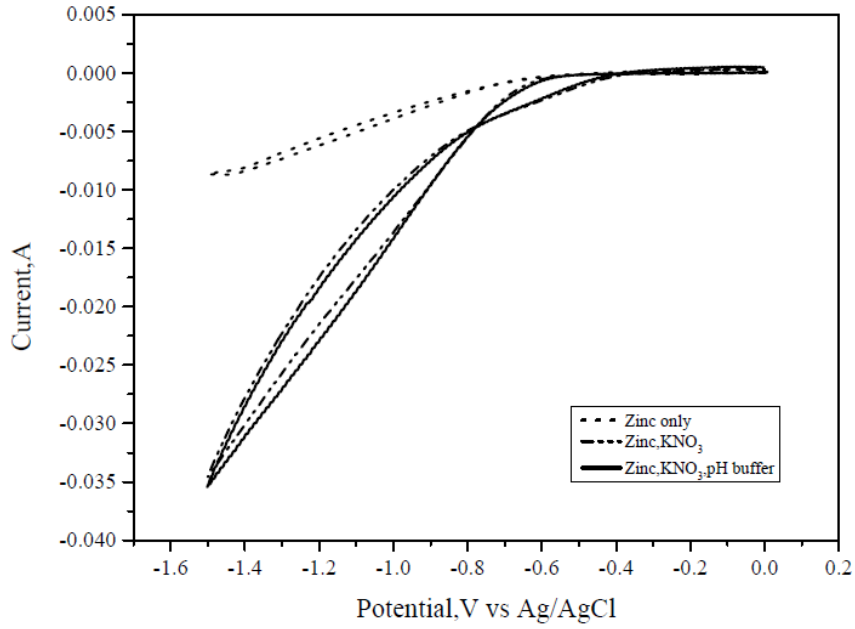

Figure 4.22: Cyclic voltammogram for 100 ppm of Zn in 0.5 M $C_6H_8O_7$

Figure 4.22 shows similar trend for 100 ppm of zinc solution with 0.5 M citric acid, with no reduction peaks present in all tested systems, was observed which could be attributed to the absence of free Zn^{2+} as a result of dominating complexation process. This in turn is generally attributed to the surface coverage of the citrate ions on the cathode surface. Such a coverage enhances the interfacial viscosity and decreases mass transfer from bulk region. At higher acid concentration, higher driving force is required regardless of applied voltage or higher Zn^{2+} concentration.

4.4 Efficiency of electrodeposition of zinc

4.4.1 Zinc in Hydrochloric acid

For 0.1 M HCl, desorption efficiencies of 64.33 %, 65.62 % and 71.34 % were achieved for 10 ppm, 50 ppm and 100 ppm, respectively as shown in Figure 4.23. The increase of Zn^{2+} concentration decreased the number of H^{+} ions in solution, thereby reducing rate of hydrogen evolution reaction as a secondary reaction.

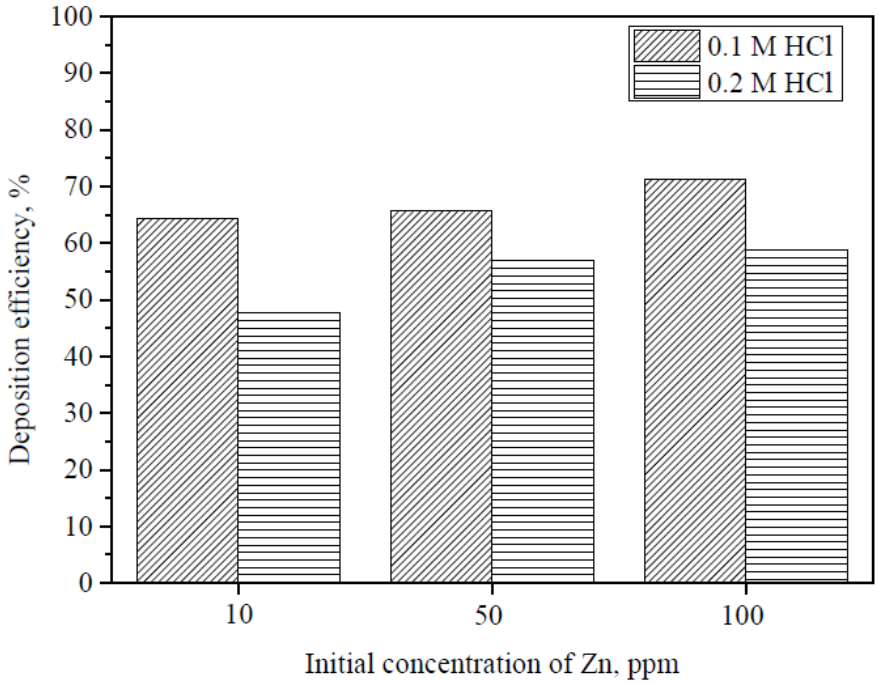

Figure 4.23: Deposition efficiency of zinc in 0.1 M and 0.2 M HCl

Complexes such as $Zn(OH)^{3-}$, $Zn(OH)_4^{2-}$, $Zn(C_8H_4O_4)_2^{2-}$, $ZnCl^{3-}$ and $ZnCl_4^{2-}$ are dissociated into zinc ions. The zinc ions will then be deposited at the stainless steel cathode. Apart from that, at 10 ppm, conductivity of zinc salt is higher causing high zinc deposition rate. Beyond 10 ppm, the conductivity decreases due to increased viscosity of the electrolyte leading to a smaller increment of zinc deposition within 10 minutes interval.

As mentioned during the CV study, the adsorption of hydrogen atom on cathode surface reduces the electrode active area and increases the resistance between the bulk electrolyte and electrode. In addition, the blocking effect induced by Cl^- ions also significantly restricts access of Zn^{2+} to the cathode surface. By increasing concentration of desorbing agent to 0.2 M, aforementioned phenomena would be intensified. Thus, it was plausible to conclude that higher acid concentration leads to a lower reduction rate.

4.4.2 Zinc in Nitric acid

Figure 4.24 depicts the percent of deposited zinc in 10 ppm, 50 ppm and 100 ppm solutions: 48.32 %, 59.37 % and 59.41 % and 42.99 %, 56.81 % and 57.82 % correspondingly, for 0.1 and 0.2 M HNO_3. Similar to HCl, it exhibits a similar trend upon increased concentration of Zn^{2+}. This is probably due to higher concentration gradient allows greater mass transport from bulk electrolyte onto stainless steel electrode.

Chloride-based electrolyte showed a higher deposition rate as compared to nitrate-based electrolyte. This could be attributed to higher number of competing reactions for the latter anion. Electroreduction of nitrate ions has been investigated by many researchers using different electrode materials; many researchers reported that stainless steel cathode shows a great selectivity towards reduction of nitrate ion to nitrite and ammonium ions. Chen, et al. (2012) reported the following reactions take place at the cathode apart from zinc ions reductions and it produces more hydroxyl anions than protons generated at anode:

$$NO_3^- + 2\bar{e} + H_2O \leftrightharpoons NO_2^- + 2OH^-$$

$$NO_3^- + 8\bar{e} + 10H_20 \leftrightharpoons NH_4^+ + 3H_20 + 10OH^-$$

$$2NO_3^- + 6H_20 + 10\bar{e} \leftrightharpoons N_2 + 12OH^-$$

$$8H_20 + 8\bar{e} \leftrightharpoons 4H_2 + 8OH^-$$

$$12H_20 \leftrightharpoons 2O_2 + 8H_3O^+ + 8\bar{e}$$

The deposition of zinc is reduced at higher concentrations of nitrate ions in electrolyte, whereby nitrites are transformed into nitric oxide in concordance to the reaction pathway shown by Lacasa, et al. (2012):

$$NO_2^- + NO_3^- + 6\bar{e} + 10H^+ \rightarrow 5H_2O + 4NO$$

This offers a quaternary side reactions preceded by zinc ions reduction, hydrogen evolution and nitrate ions reduction.

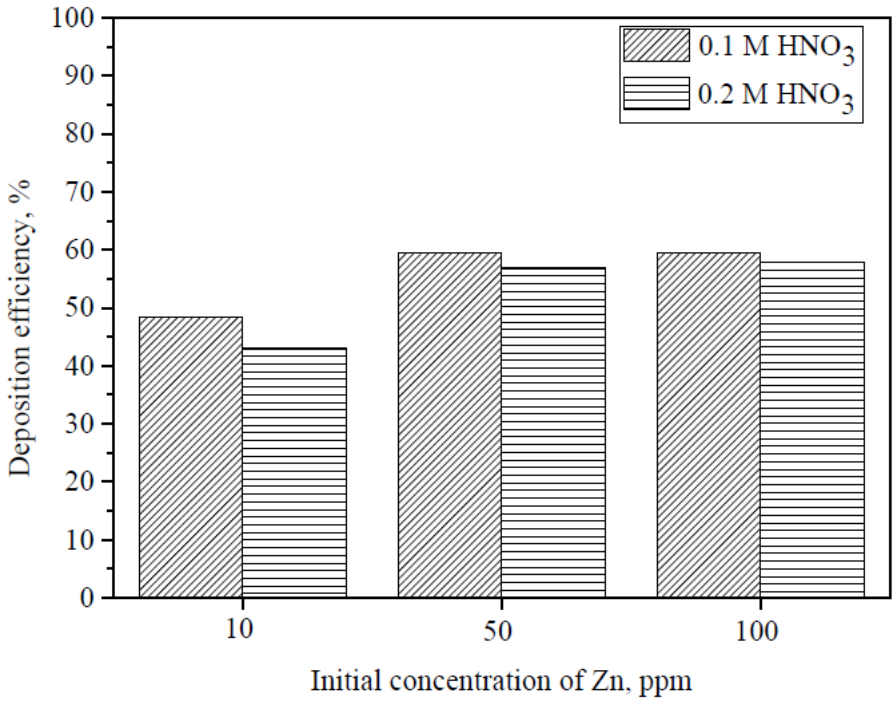

Figure 4.24: Deposition efficiency of zinc in 0.1 M and 0.2 M HNO_3

4.4.3 Zinc in Citric acid

Figure 4.25 shows the percentage of zinc deposited in 10 ppm, 50 ppm and 100 ppm solutions are 33.8 %, 43.7 %, 50.08 %; and 22.90 %, 31.21 %, 38.31 % for 0.2 M and 0.5 M citric acid, respectively. The reduction reaction of zinc, i.e. Zn^{2+}, ZnH_2Cit^{+}, ZnH_2Cit and $Zn(Cit)_2^{4-}$ increased when the concentration of Zn(II) in the electrolyte is increased (Ishizaki, et al., 2004). In view of thermodynamic perspective, the increase of zinc ions concentrations allows a positive shift of the Nernst potential for the enhancement of zinc deposition on cathode surface.

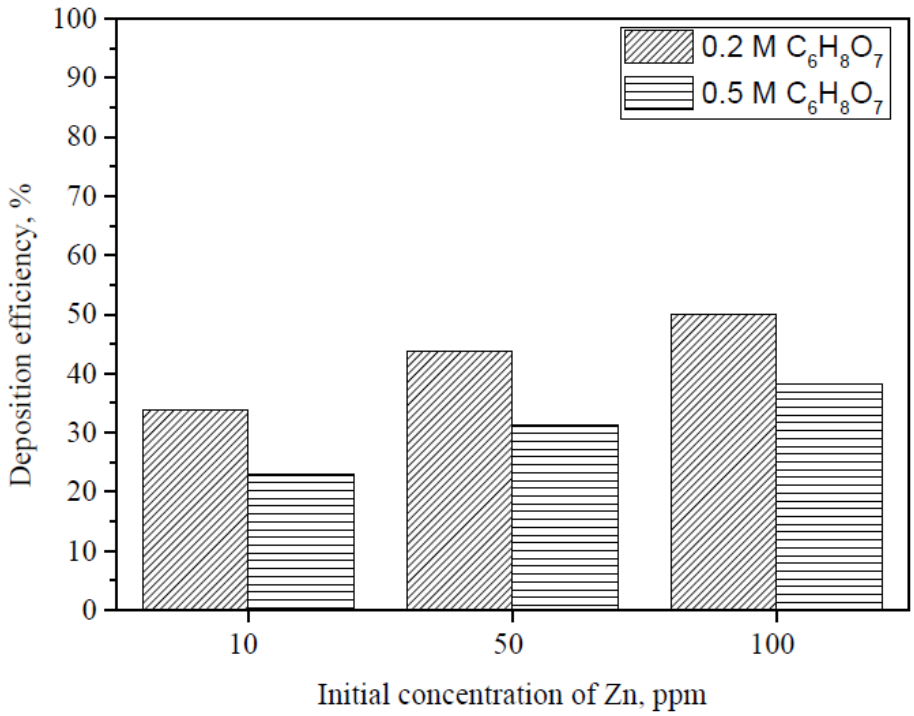

Figure 4.25: Deposition efficiency of zinc in 0.2 M and 0.5 M $C_6H_8O_7$

Reduction of Zn(II) becomes more difficult in the presence of citrate ions due to the formation of Zn(II)-citrate complex. Increased acid concentration to 0.5 M promotes the formation of non-electroactive citrate complexes, thus reducing concentration of free Zn^{2+} (Kazimierczak, et al., 2014).

Based on the obtained results, it is suggested that the best desorbing agent is 0.1 M hydrochloric acid. One of the issues that emerges from these findings is that

the concentration of zinc achievable after performing adsorption, desorption and electrodeposition is 2.472 ppm, still above the permissible discharge limit of 2 ppm for zinc in wastewater (Department of Environment, 2012). The ultimate objective of present research is to minimize the zinc level to fulfil the regulation endorsed by it. Hence, an attempt was made to prolong the deposition period to 30 minutes and to inspect the effect of doubling the current density.

4.5 Effect of deposition time

At constant applied current density of 100 A/m^2, when the deposition time was 10 minutes, the percentage of zinc deposited was 64.3 %. As the deposition time was extended to 30 minutes, it increased by 7 %. On the contrary, the amount of deposited zinc did not increased as was expected. The efficiency decreased over time as the concentration of zinc decreased and process control switched from charge transport to mass transport (Paunovic and Schlesinger, 2006). However, these findings raise intriguing questions regarding the extent to which the deposition time should be extended. After 30 minutes, the electrolyte turned into green colour indicating release of nickel and chromium ions from the stainless steel electrode (Sunada, Majima and Matsuda, 2005). The measured concentration of nickel and chromium ions were 1.045 and 1.121 ppm, respectively. The increase in dissolution rate was obvious owing to de-passivation of the stainless steel electrode surface initiated by dissolution of oxide film and breakage of uniform surface layer (Gladyshev, et al., 2013).

4.6 Effect of applied current density

Applied current density is a key operating consideration in electroreduction of zinc ions as it influences the amount of zinc deposited. At constant deposition period of 10 minutes, the percentage of zinc deposited was 64.3 % and 65.8 % with current density of 100 A/m^2 and 200 A/m^2, respectively. Contrary to the expectations, it did

not show significant increment in zinc reduction. The initial concentration of zinc electrolyte and applied current density are notably related. The electrochemical reaction happening at low initial concentration increases the effect of applied current density on the reaction rate and shifting the reaction from mass transfer-controlled reaction to a charge transfer-controlled reaction. At low current density, 100 A/m^2, there is slow consumption of zinc ions at electrode. The controlling step during the reaction period is clearly not the mass transfer of zinc ions because the initial concentration can be considered fairly low. These results reveal that electro-reduction of zinc ions is partially controlled by charge transfer. This allows production of zinc ions by complex dissociation. Meanwhile, higher current density prohibits formation of zinc complexes allowing higher reduction of zinc ions (Paunovic and Schlesinger, 2006). In other words, the increase in current density accelerates the transformation into zinc ions from complexes, which can cause higher rate of zinc deposition. A competing reaction, hydrogen evolution reaction, occurs on the cathode surface in the electrochemical cell during hydrogen ions reduction as a secondary cathodic reaction. Thus, the increase in applied current density consistently causes an increase in the rate of secondary cathodic reaction, which decreases the current efficiency.

CHAPTER 5

CONCLUSION AND RECOMMENDATIONS

5.1 Conclusion

This research project evaluated the recovery of zinc through application of adsorption, desorption and electrochemical deposition methods. The adsorption results showed that the adsorption capacity increased when initial zinc ions concentration increased from 10 to 100 ppm reaching adsorption efficiency of 98 %. Hydrochloric acid provided the highest desorption efficiency among the three desorbing agents (nitric and citric acids) for all tested Zn concentrations. However, the effect of using higher acid concentrations were different for hydrochloric and citric acids resulting in lower desorption efficiencies.

The cyclic voltammograms analysis showed no electroreduction peaks for zinc in 0.2 or 0.5 M in the citrate-based electrolyte. In contrast, chloride-based electrolyte voltammograms showed higher cathodic current and a sharper reduction peak which enhanced at higher zinc concentration.

In electrodeposition of zinc experiments, the chloride-based electrolyte showed the highest efficiency of zinc recovery that followed by the nitrate and citrate based electrolytes. Increase in acid concentration has led to the reduced zinc deposition efficiency but higher zinc concentration improved mass transfer from bulk electrolyte onto cathode surface resulting in higher zinc deposition.

Overall, the electrodeposition of zinc was successful achieving effective reduction of zinc ions concentration to meet the maximum permissible limit of zinc in wastewater of 2 ppm at the optimized deposition time and applied current density parameters.

5.2 Recommendation for Future Works

Instead of using acid for zinc desorption from PSAC, the desorption step can be carried out using deionized water as to prevent acid disposal issue to the environment. The main electrodeposition parameters such as deposition period and applied current density need to be optimized for better recovery efficiency. The prolonged deposition period will provide a better zinc recovery up to an extent whereby, the electrolyte needs to be prevented from containing excessive residual cation species dislodging from the cathode mainly chromium and nickel ions. Since the deposition period of 30 minutes has resulted the electrolyte turned into green, therefore the deposition period can be tested for five minutes interval to observe the best deposition time that does not change the colour of the electrolyte. Since the effect of doubling the applied current density did not result in a major change in percentage of zinc recovery, it can be tested with 20 A/m^2 interval between the tested values. Apart from that, type of complexing agent used serves as an important parameter. The buffer agent containing biphthalate ions, $HC_8H_4O_4^-$ has shifted the deposition potential to a more negative value requiring higher applied voltage to reduce the metal ion of interest, agent such as boric acid which is able to cover wide range of pH can be tested with an objective to reduce the metal complexes formed.

REFERENCES

Abou-Krisha, M.M., 2012. Effect of pH and current density on the electrodeposition of Zn–Ni–Fe alloys from a sulfate bath. *Journal of Coatings Technology and Research*, 9(6), pp. 775-783.

Ahmed, N.A., Eyraudb, M., Hammachea, H., Vacandiob, F., Samc, S., Gabouzec, N., Knauthb, P., Pelzerb, K. and Djeniziand, T., 2013. New insight into the mechanism of cathodic electrodeposition of zinc oxide thin films onto vitreous carbon. *Electrochimica Acta*, 94(1), pp. 238–244.

Akhtar, M., Iqbal, S., Kausar, A., Bhanger, M.I. and Shaheen, M.A., 2010. An economically viable method for the removal of selected divalent metal ions from aqueous solutions using activated rice husk. *Colloids and Surfaces B: Biointerfaces*, 75(1), pp.149-155.

Almamoori, A.M.J., Hassan, F.M. and Kassim, T.I., 2012. Impact of Industrial Wastewater on the Properties of One Major Drainage in the Region of the Middle Euphrates/Iraq. *International Journal of Chemical Sciences*, 10(4), pp. 1785-1798.

Amuda, O.S., Giwa, A. and Bello, I.A., 2007. Removal of heavy metal from industrial wastewater using modified activated coconut shell carbon. *Biochemical Engineering Journal*, 36(2), pp.174-181.

Annadurai, G., Juang, R.S. and Lee, D.J., 2003. Adsorption of heavy metals from water using banana and orange peels. *Water Science & Technology*, 47(1), pp.185-190.

Barbalace, L., 2015. *Periodic Table of Elements*. [online] Available at: <http://EnvironmentalChemistry.com/yogi/periodic/>[Accessed 21 December 2015].

Bedir, M., Korkmaz, D., Bakkaloglu, O.F., Oztas, M., Karahan, İ.H. and Haciibrahimoglu, M.Y., 2015. Effect of pH Values on the Characterization of Electrodeposited Zn–Mn Coatings in Chloride-Based Acidic Environment. *International Journal of Electrochemical Science*, 10(1), pp.4513-4522.

Bhatt, R. R. and Shah, B.A., 2013. Sorption studies of heavy metal ions by salicylic acid–formaldehyde–catechol terpolymeric resin: Isotherm, kinetic and thermodynamics. *Arabian Journal of Chemistry*, 8(1), pp. 414–426.

Bockris, J. O. M., Nagy, Z. and Danjanovic, A., 1972. On the deposition and dissolution of zinc in alkaline solutions. *Journal of the electrochemical society*, 119(1), pp. 285-295.

Booran, S.K., Doan, H.D. and Lohi, A., 2015. Recovery of Zn(II) and Ni(II) Binary from Wastewater Using Integrated Biosorption and Electrodeposition. *CLEAN–Soil, Air, Water*, 43(3), pp. 368-374.

Bux, F., Swalaha, F.M. and Kasan, H.C., 1995. Assessment of acids as desorbents of metal ions bound to sludge surfaces. *Water SA*, 21(4), pp. 319-324.

Chen, S. K., 2012. *Biomodification of palm shell activated carbon using Aspergillus niger and Bacillus subtilis*. Master. Universiti Tunku Abdul Rahman. Available at: <http://eprints.utar.edu.my/958/1/SCA-2013-1001675-1.pdf> [Accessed 21 December 2015].

Chen, F.Y., Liu, J.G., Chen, H. and Yan, C.W., 2012. Study on Hydrogen Evolution Reaction at a Graphite Electrode in the All-Vanadium Redox Flow Battery. *International Journal of Electrochemical Science*, 7(1), pp. 3750-3764.

Chorkendorff, I. and Niemantsverdriet, J.W., 2006. *Concepts of modern catalysis and kinetics*. John Wiley & Sons.

Chu, K.H. and Hashim, M.A., 2002. Adsorption and desorption characteristics of zinc on ash particles derived from oil palm waste. *Journal of chemical Technology and Biotechnology*, *77*(6), pp.685-693.

Chun-rong, W., Xin, R., Wen-xiu, L., Zhi-Fei, H., Chao, K. and Qi, G., 2013. Adsorption of Zinc and Copper Heavy Metal Ions from Smelting Wastewater Using Modified Lava Particles. *Polish Journal of Environmental Studies*, 22(6), pp. 1863-1869.

Colli, A.N. and Bisang, J.M., 2014. Comparison of the performance of flow-by three-dimensional cylindrical electrochemical reactors with inner or outer counter electrode under limiting current conditions. *Electrochimica Acta*, 154(1), pp. 468–475.

Dabrowski, A., 2001. Adsorption- from theory to practice. *Advances in Colloid and Interface Science*, 93(1), pp. 135-224.

Deepatana, A. and Valix, M., 2004. Adsorption of Metals from Metal-Organic Complexes Derived from Bioleaching of Nickel Laterite Ores. *ECI Digital Archives*, 21(1), pp. 18-25.

Department of Environment (DOE), 2012. Malaysia Environmental Quality Report, Ministry of Science, Technology and the Environment, Malaysia. ISSN 0127-6433.

Dupont, L., Bouanda, J., Dumonceau, J. and Aplincourt, M., 2005. Biosorption of Cu (II) and Zn (II) onto a lignocellulosic substrate extracted from wheat bran. *Environmental Chemistry Letters*, 2(4), pp.165-168.

El-Said, A.G., Badawy, N.A., Abdel-Aal, A.Y. and Garamon, S.E., 2011. Optimization parameters for adsorption and desorption of Zn (II) and Se (IV) using rice husk ash: kinetics and equilibrium. *Ionics*, 17(3), pp.263-270.

El-Shafey, E.I., 2010. Removal of Zn (II) and Hg (II) from aqueous solution on a carbonaceous sorbent chemically prepared from rice husk. *Journal of hazardous materials*, 175(1), pp.319-327.

Ferro-Garcia, M.A., Rivera-Utrilla, J., Rodriguez-Gordillo, J. and Bautista-Toledo, I., 1988. Adsorption of zinc, cadmium, and copper on activated carbons obtained from agricultural by-products. *Carbon*, 26(3), pp.363-373.

Fleischmann, M., Oldfield, J.W. and Tennakoon, L., 1971. Fluidized bed electrodes Part IV. Electrodeposition of copper in a fluidized bed of copper-coated spheres. *Journal of Applied Electrochemistry*, 1(2), pp. 103-112.

Gabe, D.R., 1978. *Principles of metal surface treatment and protection*. Pergamon Press.

Galla, U., Juttner, K. and Schmieder, H., 2000. Electrochemical approaches to environmental problems in the process industry. *Electrochimica Acta*, 45(15), pp. 2575–2594.

Gamburg, Y.D. and Zangari, G., 2011. *Theory and Practice of Metal Electrodeposition*. New York: Springer.

Gladyshev, S.V., Abdulvaliev, R.A., Beisembekova, K.O. and Sarsenbay, G., 2013. Study of Gallium Plating of Metal Electrodes. *Journal of Materials Science and Chemical Engineering*, 1(5), pp. 39-45.

Gurevich, Y.U., 1989. Influence of a Secondary Process on Copper Deposition Rate in Nitrate Baths. *Soviet Electrochemistry*, 25(6), pp. 698-700.

Gupta, V. K. and Ali, I., 2004. Removal of lead and chromium from wastewater using bagasse fly ash-A low sugar industry waste. *Journal of colloid and interface science*, 271(2), pp. 321-328.

Gupta, V. K. and Sharma, S., 2003. Removal of Zinc from Aqueous Solutions Using Bagasse Fly Ash-A Low Cost Adsorbent. *Industrial & engineering chemistry research*, 42(25), pp. 6619-6624.

Gupta, V. K., Nayak, A., Bhushan, N. and Agarwal, S., 2015. A critical analysis on the Efficiency of Activated Carbons from Low-Cost Precursors for Heavy Metals Remediation. *Critical Reviews in Environmental Science and Technology*, 45(6), pp. 613-668.

Gustafsson, J.P., 2014. *Visual MINTEQ, Version 3.1*. [online] Available at: <http://www2. lwr. kth. se/English/Oursoftware/vminteq>. [Accessed 3 January 2016].

Hankin, A. and Kelsall, G. H., 2012. Electrochemical recovery of nickel from nickel sulfamate plating effluents. *Journal of Applied Electrochemistry*, 42(9), pp. 629–643.

Hatfield, T.L., Kleven, T. L. and Pierce, D. T., 1995. Electrochemical remediation of metal-bearing wastewaters Part 1: Copper removal from simulated mine drainage waters. *Journal of Applied Electrochemistry*, 26(6), pp. 567-574.

Haynes, W. M., 2014. *CRC handbook of chemistry and physics*. CRC press.

Hesas, R. H., Daud, W.M.A.W., Sahu, J. N. and Niyya, A. A., 2013. The effects of a microwave heating method on the production of activated carbon from agricultural waste: A review. *Journal of Analytical and Applied pyrolysis*, 100(1), pp. 1-11.

Horányi, G., 1996. Adsorption of Cl^- ions on electrodeposited rhodium black layer (rhodized electrode) at low concentrations. *Reaction Kinetics and Catalysis Letters*, 59(2), pp. 211-217.

Horsfall, M.J., Arbia, A.A. and Spiff, A.I., 2004. Removal of Cu (II) and Zn (II) ions from wastewater by cassava (Manihot esculenta Cranz) waste biomass. *African Journal of Biotechnology*, 2(10), pp.360-364.

International Lead and Zinc Study Group (ILZSG), 2015. *Lead and Zinc Statistics.* [online] Available at: < http://www.ilzsg.org/static/statistics.aspx > [Assessed 18 June 2015].

International Trade Centre, 2014. *Natural rubber exports by country*. [online] Available at: <http://www.worldstopexports.com/natural-rubber-exports-country/3354 > [Accessed 9 May 2015].

Ipeaiyeda, A. R. and Tesi, G.O., 2014. Sorption and Desorption Studies on Toxic Metals From Brewery Effluent Using Eggshell as Adsorbent. *Advances in Natural Science*, 7(2), pp. 15-24.

Iqbal, M., Saeed, A. and Kalim, I., 2009. Characterization of adsorptive capacity and investigation of mechanism of Cu^{2+}, Ni^{2+} and Zn^{2+} adsorption on mango peel waste from constituted metal solution and genuine electroplating effluent. *Separation Science and Technology*, 44(15), pp.3770-3791.

Ishizaki, T., Ohtomo, T., Sakamoto, Y. and Fuwa, A., 2004. Effect of pH on the electrodeposition of ZnTe film from a citric acid solution. *Materials Transactions*, 45(2), pp. 277-280.

Issabayeva, G. and Aroua, M.K., 2011. Removal of copper and zinc ions onto biomodified palm shell activated carbon. *World Academy of Science, Engineering and Technology*, 76(1), pp.259-262.

Issabayeva, G., Aroua, M.K. and Sulaiman, N.M.N., 2006. Removal of lead from aqueous solutions on palm shell activated carbon. *Bioresource Technology*, 97(18), pp. 2350-2355.

Kavitha, B., Santhosh, P., Renukadevi, M., Kalpana, A., Shakkthivel, P. and Vasudevan, T., 2006. Role of organic additives on zinc plating. *Surface and Coatings Technology*, 201(6), pp. 3438-3442.

Kazimierczak, H., Ozga, P., Jałowiec, A. and Kowalik, R., 2014. Tin–zinc alloy electrodeposition from aqueous citrate baths. *Surface and Coatings Technology*, 240(1), pp. 311-319.

Konstantinos, D., Achilleas, C. and Valsamidou, V., 2011. Removal of Nickel, Copper, Zinc and Chromium from Synthetic and Industrial Wastewater by Electrocoagulation. *International Journal of Environmental Sciences*, 1(5), pp. 698-703.

Krishnan, R. M., Kennedy, C. J., Jayakrishnan, S., Sriveeraraghavan, S. and Natarajan, S. R., 1996. Zinc Electrodeposition from Acetate Solutions. *Metal Finishing*, 94(10), pp. 43-46.

Kumar, P.S., 2013. Adsorption of Zn (II) ions from aqueous environment by surface modified Strychnos potatorum seeds, a low cost adsorbent. *Polish Journal of Chemical Technology*, 15(3), pp.35-41.

Kumar, Y. P., Vijetha, P., Kumaraswamy, K., Pallavi, P., Rao, K. V., Kumar, T. A., Mariadas, K. and Kalyani, G., 2010. Adsorption of Zinc by Natural Adsorbent Bentonite – a Clay Material. *International Journal of Applied Environmental Sciences*, 5(4), pp. 581–589.

Kushwaha, S. and Sudhakar, P., 2013. Sorption mechanism of Cd (II) and Zn (II) onto modified palm shell. *Adsorption Science & Technology*, 31(6), pp.503-520.

Kyzas, G.Z. and Kostoglou, M., 2014. Green Adsorbents for Wastewaters: A Critical Review. *Materials*, 7(1), pp. 333-364.

Lacasa, E., Canizares, P., Llanos, J. and Rodrigo, M.A., 2012. Effect of the cathode material on the removal of nitrates by electrolysis in non-chloride media. *Journal of hazardous materials*, 213(1), pp.478-484.

Li, C.Q., Li, X.H., Wang, Z.X. and Guo, H.J., 2007. Nickel electrodeposition from novel citrate bath. *Transactions of Nonferrous Metals Society of China*, 17(6), pp. 1300-1306.

Li, Z., Xiang, Y. and Tong, A., 2008. Ratiometric chemosensor for fluorescent determination of Zn^{2+} in aqueous ethanol. *Analytica chimica acta*, 619(1), pp. 75-80.

Madhava Rao, M., Chandra Rao, G. P., Seshaiah, K., Choudary, N. V. and Wang, M.C., 2007. Activated carbon from Ceiba pentandra hulls, an agricultural waste, as an adsorbent in the removal of lead and zinc from aqueous solutions. *Waste Management*, 28(5), pp. 849-858.

Malaysia Palm Oil Council., 2014. *One of The World's Largest Palm Oil Exporter*. [online] Available at: <http://www.mpoc.org.my/Malaysian_Palm_Oil_Industry.aspx> [Accessed 9 May 2015].

Manzano, C.V., Alegre, D., Caballero-Calero, O., Alén, B. and Martín-González, M.S., 2011. Synthesis and luminescence properties of electrodeposited ZnO films. *Journal of Applied Physics*, 110(4), pp. 043531-043538.

Mehta, P. and Sindal, R., 2010. Study of Zn(II) in Different Sodium Salts as Supporting Electrolytes using Cyclic Voltammetric Technique. *International Journal of Chemical Sciences*, 8(3), pp. 1511-1516.

Mendoza-Huízar, L. H., Rios-Reyes, C. H. and Gómez-Villegas, M. G., 2010. Zinc Electrodeposition from Chloride Solutions onto Glassy Carbon Electrode. *Journal of the Mexican Chemical Society*, 53(4), pp. 243-247.

Mishra, P.C. and Patel, R.K., 2009. Removal of lead and zinc ions from water by low cost adsorbents. *Journal of Hazardous Materials*, 168(1), pp.319-325.

Mo, Y., Huang, Q., Li, W., Hu, S., Huang, M. and Huang, Y., 2011. Effect of sodium benzoate on zinc electrodeposition in chloride solution. *Journal of Applied Electrochemistry*, 41(7), pp. 859-865.

Moezzi, A., McDonagh, A.M. and Cortie, M.B., 2012. Zinc oxide particles: Synthesis, properties and applications. *Chemical Engineering Journal*, 185(1), pp. 1-22.

Mohamed, M. and Yap, C.Y., 2006. An electrogenerative process for the recovery of gold from cyanide solutions. *Chemosphere*, 67(8), pp. 1502–1510.

Mohammad, M., Maitra, S., Ahmad, N., Bustam, A., Sen, T.K. and Dutta, B.K., 2010. Metal ion removal from aqueous solution using physic seed hull. *Journal of hazardous materials*, 179(1), pp.363-372.

Mohammod, M., Maitra, S., Sen, T.K. and Dutta, B.K., 2010. Removal of Zn^{2+} from Aqueous Solution using Castor Seed Hull. *Water, Air, Soil Pollution*, 215(1), pp. 609–620.

Morrow, H., 1986. *Encyclopedia of Materials Science and Engineering*, Vol. 7, M. B. Bever (ed.), MIT Press, Cambridge, Massachusetts.

Naiya, T.K., Chowdhury, P., Bhattacharya, A.K. and Das, S.K., 2009. Saw dust and neem bark as low-cost natural biosorbent for adsorptive removal of Zn (II) and Cd (II) ions from aqueous solutions. *Chemical Engineering Journal*, 148(1), pp.68-79.

Najafi, N.M., Shakeri, P. and Ghasemi, E., 2010. Separation and Preconcentration of Ultra Traces of Some Heavy Metals in Environmental Samples by Electrodeposition Technique Prior to Flame Atomic Absorption Spectroscopy Determination (ED-FAAS). *Transactions C: Chemistry and Chemical Engineering*, 17(2), pp. 144-151.

Nasernejad, B., Zadeh, T.E., Pour, B.B., Bygi, M.E. and Zamani, A., 2005. Camparison for biosorption modeling of heavy metals (Cr (III), Cu (II), Zn (II)) adsorption from wastewater by carrot residues. *Process Biochemistry*, 40(3), pp.1319-1322.

Njoku, V.O., 2014. Biosorption potential of cocoa pod husk for the removal of Zn (II) from aqueous phase. *Journal of Environmental Chemical Engineering*, 2(2), pp.881-887.

Panda, B., 2013. Effects of Added Chloride Ion on Electrodeposition of Copper from a Simulated Acidic Sulfate Bath Containing Cobalt Ions. *ISRN Metallurgy*, 2013.

Paunovic, M. and Schlesinger., 2006. *Fundamentals of Electrochemical Deposition*. Hoboken, New Jersey. John Wiley & Son Inc.

Pletcher, D., Whyte, I., Walsh, F.C. and Millington, J. P., 1991. Reticulated vitreous carbon cathodes for metal ion removal from process streams Part I: Mass transport studies. *Journal of applied electrochemistry*, 21(8), pp. 659-666.

Popoola, A.P.I. and Fayomi, O.S., 2011. Performance evaluation of zinc deposited mild steel in chloride medium. *International Journal of Environmental Sciences*, 6(1), pp.3254-3263.

Qingwei, G., Qiongfang, Z., Wenjie, X., Yanfei, W. and Zhencheng, X., 2014. Electrochemical Recovery of Metals from Cadmium Wastewater. *Chemistry Letters*, 43(8), pp. 1312-1314.

Oliveira, W.E., Franca, A.S., Oliveira, L.S. and Rocha, S.D., 2008. Untreated coffee husks as biosorbents for the removal of heavy metals from aqueous solutions. *Journal of Hazardous Materials*, 152(3), pp.1073-1081.

Radzimska, A.K. and Jesionowski, T., 2014. Zinc Oxide - From Synthesis to Application: A Review. *Materials*, 7(4), pp. 2833-2881.

Rao, M.M., Ramana, D.K., Seshaiah, K., Wang, M.C. and Chien, S.C., 2009. Removal of some metal ions by activated carbon prepared from Phaseolus aureus hulls. *Journal of hazardous materials*, 166(2), pp.1006-1013.

Reddad, Z., Gerente, C., Andres, Y. and LeCloirec, P., 2002. Adsorption of several metal ions onto a low-cost biosorbent: kinetic and equilibrium studies. *Environmental Science and Technology*, 36(9), pp. 2067–2073.

Ruetschi, P., 1967. Solubility and diffusion of hydrogen in strong electrolytes and the generation and consumption of hydrogen in sealed primary batteries. *Journal of applied electrochemistry*, 114(4), pp. 301-305.

Rose, P.K. and Devi, R., 2015. Adsorption Isotherm Study of Cadmium on Dairy Sludge Based Adsorbent. *International Journal for Innovative Research in Science and Technology*, 1(11), pp. 145-151.

Ruthven, D.M., 1984. *Principles of Adsorption and Adsorption Processes.* Canada: John Wiley & Son Inc.

Salam, O.E.A., Reiad, N.A. and ElShafei, M.M., 2011. A study of the removal characteristics of heavy metals from wastewater by low-cost adsorbents. *Journal of Advanced Research*, 2(4), pp. 297-303.

Sen, T.K. and Khoo, C., 2013. Adsorption Characteristics of Zinc (Zn 2+) from Aqueous Solution by Natural Bentonite and Kaolin Clay Minerals: A Comparative Study. *Computational Water, Energy, and Environmental Engineering*, *2*(3), pp.1-6.

Shaikh, A. A., Firdaws, J., Badrunnessa, S., Serajee, S., Rahman, M. S. and Bakshi, P.K., 2011. Electrochemical Studies of the pH Dependence of Cu(II) Reduction in Aqueous Britton-Robinson Buffer Solution. *International of Electrochemical Science*, 6(1), pp. 2333–2343.

Sharma, S.K., 2011. *Green corrosion chemistry and engineering: opportunities and challenges*. John Wiley & Sons.

Shrestha, S., Son, G., Lee, S.H. and Lee, T.G., 2013. Isotherm and thermodynamic studies of Zn (II) adsorption on lignite and coconut shell-based activated carbon fiber. *Chemosphere*, 92(8), pp.1053-1061.

Srivastava, V.C., Mall, I.D. and Misha, I.M., 2006. Characterisation of mesoporous rice husk ash (RHA) and adsorption kinetics of metal ions from aqueous solution onto RHA. *Journal of Hazardous Materials*, 134(1), pp. 257-267.

Stankovic´, V., 2012. Electrochemical engineering – its appearance, evolution and present status. Approaching an anniversary. *Journal of Electrochemical Science and Engineering*, 2(2), pp. 67–75.

Statista, 2015. *Global consumption of zinc from 2004 to 2014 (in 1,000 metric tons)*. [online] Available at: < http://www.statista.com/statistics/264884/world-zinc-usage/> [Accessed 10 August 2015].

Sunada, S., Majima, K. and Matsuda, T., 2005. Dissolution Behavior of SUS304 Stainless Steel due to General Corrosion in H_2SO_4-NaCl Aqueous Solution. *粉体および粉末冶金*, 52(7), pp. 530-536.

Thakur, L.S. and Parmar, M., 2013. Adsorption of Heavy Metal (Cu^{2+}, Ni^{2+} and Zn^{2+}) from Synthetic Waste Water by Tea Waste Adsorbent. *International Journal of Chemical and Physical Sciences*, 2(6), pp. 621-629.

Tuaweri, T. J., Adigio, E. M. and Jombo, P. P., 2013. A Study of Process Parameters for Zinc Electrodeposition from a Sulphate Bath. *International Journal of Engineering Science Invention*, 2(8), pp. 17-24.

Vazquez, G., Gonzalez, J., Freire, M., Calvo, M. and Antorrena, G., 2009. Determination of the optimal conditions for the adsorption of cadmium ions and phenol on chestnut (castanea sativa) shell. *Globa NEST Journal*, 11(2), pp. 196-204.

Volesky, B. and Holan, Z.R., 1995. Biosorption of Heavy Metals. *Biotechnology Progress*, 11(3), pp. 235-250.

Wasewar, K.L., 2010. Adsorption of metals onto tea factory waste: A review. *International Journal of Research and Reviews in Applied Sciences*, 3(3), pp. 303-322.

World Health Organization (WHO), 2000. Global *Water Supply and Sanitation Assessment Report 2000*, Geneva, Switzerland.

Yang, R.T, 2003. *Adsorbents: Fundamental and Applications*. John Wiley & Sons, Inc. Hoboken, New Jersey.

Yao, G., Zhang, M., Lv, J., Xu, K., Shi, S., Gong, Z., Tao, J., Jiang, X., Yang, L., Cheng, Y. and He, G., 2015. Effects of Electrodeposition Electrolyte Concentration on Microstructure, Optical Properties and Wettability of ZnO Nanorods. *Journal of The Electrochemical Society*, 162(7), pp.300-304.

Ye, H., Zhu, Q. and Du, D., 2010. Adsorptive removal of Cd (II) aqueous solution using natural and modified rice husk. *Bioresource Technology*, 101(14), pp. 5175–5179.

Yoshida, T., Komatsu, D., Shimokawa, N. and Minoura, H., 2004. Mechanism of cathodic electrodeposition of zinc oxide thin films from aqueous zinc nitrate baths. *Thin solid films*, 451(1), pp. 166-169.

Zhang, X.G., 1996. *Corrosion and Electrochemistry of Zinc.* Plenum Press, New York.